

## Article

# IL-15, gluten and HLA-DQ8 drive tissue destruction in coeliac disease

<https://doi.org/10.1038/s41586-020-2003-8>

Received: 30 October 2018

Accepted: 16 December 2019

Published online: 12 February 2020

 Check for updates

Valérie Abadie<sup>1,2,3,19</sup>✉, Sangman M. Kim<sup>3,4,5,19</sup>, Thomas Lejeune<sup>1,2,19</sup>, Brad A. Palanski<sup>6</sup>, Jordan D. Ernest<sup>3,4</sup>, Olivier Taster<sup>7</sup>, Jordan Voisine<sup>3,4</sup>, Valentina Discepolo<sup>3</sup>, Eric V. Marietta<sup>8,9,10</sup>, Mohamed B. F. Hawash<sup>7,11</sup>, Cezary Ciszewski<sup>3,4</sup>, Romain Bouziat<sup>3,4</sup>, Kaushik Panigrahi<sup>3</sup>, Irina Horwath<sup>8</sup>, Matthew A. Zurenski<sup>3</sup>, Ian Lawrence<sup>3</sup>, Anne Dumaine<sup>7</sup>, Vania Yotova<sup>7</sup>, Jean-Christophe Grenier<sup>7</sup>, Joseph A. Murray<sup>8</sup>, Chaitan Khosla<sup>6,12,13</sup>, Luis B. Barreiro<sup>7,14,15</sup> & Bana Jabri<sup>3,4,16,17,18</sup>✉

Coeliac disease is a complex, polygenic inflammatory enteropathy caused by exposure to dietary gluten that occurs in a subset of genetically susceptible individuals who express either the HLA-DQ8 or HLA-DQ2 haplotypes<sup>1,2</sup>. The need to develop non-dietary treatments is now widely recognized<sup>3</sup>, but no pathophysiologically relevant gluten- and HLA-dependent preclinical model exists. Furthermore, although studies in humans have led to major advances in our understanding of the pathogenesis of coeliac disease<sup>4</sup>, the respective roles of disease-predisposing HLA molecules, and of adaptive and innate immunity in the development of tissue damage, have not been directly demonstrated. Here we describe a mouse model that reproduces the overexpression of interleukin-15 (IL-15) in the gut epithelium and lamina propria that is characteristic of active coeliac disease, expresses the predisposing HLA-DQ8 molecule, and develops villous atrophy after ingestion of gluten. Overexpression of IL-15 in both the epithelium and the lamina propria is required for the development of villous atrophy, which demonstrates the location-dependent central role of IL-15 in the pathogenesis of coeliac disease. In addition, CD4<sup>+</sup> T cells and HLA-DQ8 have a crucial role in the licensing of cytotoxic T cells to mediate intestinal epithelial cell lysis. We also demonstrate a role for the cytokine interferon-γ (IFNγ) and the enzyme transglutaminase 2 (TG2) in tissue destruction. By reflecting the complex interaction between gluten, genetics and IL-15-driven tissue inflammation, this mouse model provides the opportunity to both increase our understanding of coeliac disease, and develop new therapeutic strategies.

Coeliac disease is characterized by dietary gluten-induced destruction of the small intestinal epithelium and a substantial infiltration of intraepithelial lymphocytes (IELs)<sup>5</sup>. The presence of IgG antibodies against deamidated gliadin peptides (DGPs) and anti-TG2 IgG and IgA antibodies are hallmarks of active coeliac disease that are used for diagnosis of patients<sup>5,6</sup>.

The mechanisms underlying the clinical spectrum of coeliac disease remain poorly understood<sup>5</sup>. IL-15 is a pro-inflammatory cytokine that is presented by its private chain IL-15Rα on the cell surface under conditions of stress and inflammation<sup>7,8</sup>. In active coeliac disease, IL-15

is upregulated in both the lamina propria and in intestinal epithelial cells (IECs). IL-15 expressed by IECs has a crucial role in the expansion of IELs with a cytotoxic phenotype in patients with coeliac disease<sup>9</sup>. In addition, studies in gluten-immunized mouse models suggest that gluten-specific CD4<sup>+</sup> T cells are not sufficient to induce villous atrophy<sup>10</sup>. These observations previously led us to propose a model in which the combination of adaptive anti-gluten immunity and IL-15 overexpression in IECs is required for CD8<sup>+</sup> cytotoxic intraepithelial T cells (IE-CTLs) to mediate tissue destruction by acquiring a fully activated killer phenotype<sup>11</sup>. In keeping with this hypothesis, potential patients

<sup>1</sup>Department of Microbiology, Infectiology, and Immunology, Faculty of Medicine, University of Montreal, Montreal, Quebec, Canada. <sup>2</sup>Sainte-Justine Hospital Research Centre, University of Montreal, Montreal, Quebec, Canada. <sup>3</sup>Department of Medicine, University of Chicago, Chicago, IL, USA. <sup>4</sup>Committee on Immunology, University of Chicago, Chicago, IL, USA. <sup>5</sup>Department of Biology, University of San Francisco, San Francisco, CA, USA. <sup>6</sup>Department of Chemistry, Stanford University, Stanford, CA, USA. <sup>7</sup>Department of Genetics, Sainte-Justine Hospital Research Centre, University of Montreal, Montreal, Quebec, Canada. <sup>8</sup>Division of Gastroenterology and Hepatology, Mayo Clinic, Rochester, MN, USA. <sup>9</sup>Department of Immunology, Mayo Clinic, Rochester, MN, USA. <sup>10</sup>Department of Dermatology, Mayo Clinic, Rochester, MN, USA. <sup>11</sup>Department of Biochemistry, Faculty of Medicine, University of Montreal, Montreal, Quebec, Canada. <sup>12</sup>Department of Chemical Engineering, Stanford University, Stanford, CA, USA. <sup>13</sup>Stanford ChEM-H, Stanford University, Stanford, CA, USA. <sup>14</sup>Department of Pediatrics, Faculty of Medicine, University of Montreal, Montreal, Quebec, Canada. <sup>15</sup>Department of Medicine, Section of Genetic Medicine, University of Chicago, Chicago, IL, USA. <sup>16</sup>Department of Pediatrics, Section of Gastroenterology, Hepatology and Nutrition, University of Chicago, Chicago, IL, USA. <sup>17</sup>Department of Pathology, University of Chicago, Chicago, IL, USA. <sup>18</sup>University of Chicago Celiac Disease Center, University of Chicago, Chicago, IL, USA. <sup>19</sup>These authors contributed equally: Valérie Abadie, Sangman M. Kim, Thomas Lejeune. ✉e-mail: vabadie@medicinebsd.uchicago.edu; bjabri@bsd.uchicago.edu

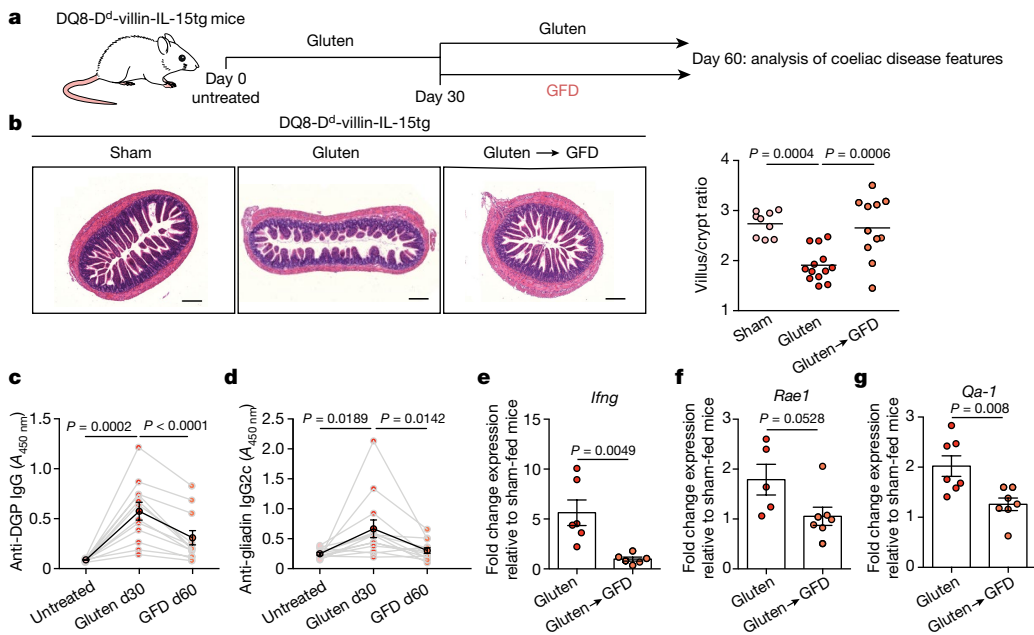


**Fig. 1 | DQ8-D<sup>d</sup>-villin-IL-15tg mice: a gluten-dependent model of coeliac disease with villous atrophy.** **a–g**, DQ8-D<sup>d</sup>-villin-IL-15tg mice were maintained on a gluten-free diet (GFD; sham), fed gluten for 60 days (gluten), or fed gluten for 30 days and then reverted to a GFD (gluten→GFD) for 30 days. **a**, Experimental timeline. **b**, Left, haematoxylin and eosin (H&E) staining of paraffin-embedded ileum sections. Scale bars, 200 μm. Right, graph depicts the ratio of the morphometric assessment of villus height to crypt depth (GFD,  $n=9$ ; gluten,  $n=13$ ; gluten→GFD,  $n=11$  mice). **c**, Serum levels of anti-DGP IgG antibodies were measured by ELISA. Serum was collected sequentially in the same mice ( $n=12$ ) before gluten feeding (untreated), 30 days after gluten feeding (gluten d30), and 30 days after reversion to a GFD (GFD d60). **d**, Serum

levels of anti-gliadin IgG2c antibodies, measured as in **c** ( $n=12$  mice per group). **e**, Expression of *Ifng* in the lamina propria was measured by quantitative PCR (qPCR). Relative expression levels in gluten-fed ( $n=6$ ) and gluten→GFD ( $n=6$ ) mice were normalized against the expression levels observed in sham-fed DQ8-D<sup>d</sup>-villin-IL-15tg mice. **f**, **g**, Expression of *Rae1* (gluten,  $n=5$ ; gluten→GFD,  $n=7$ ) (**f**) and *Qa-1* (also known as *H2-T23*) (gluten,  $n=7$ ; gluten→GFD,  $n=7$ ) (**g**) in the intestinal epithelium measured by qPCR as in **e**. Data are mean values (**b**) or mean ± s.e.m. (**c–g**) from four (**b–d**) or two (**e–g**) independent experiments. *P* values determined by analysis of variance (ANOVA) with Tukey's multiple comparison (**b**) or paired (**c, d**) or unpaired (**e–g**) two-tailed *t*-test.

with coeliac disease who conserve a normal intestinal morphology despite having lost oral tolerance to gluten, lack upregulation of IL-15 in IECs<sup>9</sup>. Furthermore, studies using ovalbumin as a model dietary antigen and transgenic mice with CD4<sup>+</sup> T cells specific for ovalbumin, showed that the cooperation between IL-15 and CD4<sup>+</sup> T cells is crucial to activate CD8<sup>+</sup> T cells and induce tissue damage<sup>12</sup>.

To define the pathophysiological role of IL-15 in the different mucosal compartments, we studied mice that overexpress IL-15 in IECs, the lamina propria, or both. Transgenic DQ8-D<sup>d</sup>-IL-15tg mice that overexpress IL-15 under the major histocompatibility complex (MHC) class I promoter D<sup>d</sup>, which drives IL-15 upregulation in the lamina propria and mesenteric lymph nodes, but not in IECs, developed T helper 1 (T<sub>H</sub>1) immunity to gluten and anti-DGP antibodies without altering the cytolytic phenotype of IELs<sup>13</sup> (Extended Data Figs. 1a–d, 2). By contrast, DQ8-villin-IL-15tg mice that overexpress IL-15 in IECs under the intestinal epithelium-specific villin promoter were unable to develop adaptive anti-gluten immunity, as assessed by the absence of anti-gliadin IgG2c (Extended Data Fig. 1b) and anti-DGP antibodies (Extended Data Fig. 1c). However, they displayed an expansion of IELs with high levels of granzyme B and perforin expression (Extended Data Fig. 2e–g, j). Notably, neither DQ8-D<sup>d</sup>-IL-15tg nor DQ8-villin-IL-15tg mice developed villous atrophy (Extended Data Fig. 1e).

To test the hypothesis that IL-15 upregulation in both IECs and the lamina propria is required for the development of villous atrophy, we generated DQ8-D<sup>d</sup>-villin-IL-15tg mice. Approximately 75% of DQ8-D<sup>d</sup>-villin-IL-15tg mice developed small intestinal tissue destruction after 30 days of gluten feeding (Extended Data Figs. 1e, 3a, b). Notably, the villous architecture was restored after the exclusion of gluten (Fig. 1a, b). Furthermore, as in patients with coeliac disease, gluten-fed DQ8-D<sup>d</sup>-villin-IL-15tg mice developed plasmacytosis in the lamina

propria (Extended Data Figs. 3c, 4a), and had circulating anti-gliadin IgG and IgA antibodies (Extended Data Fig. 4b, c) and anti-DGP IgG antibodies (Fig. 1c, Extended Data Fig. 3d). Although we could detect co-localization of IgA and TG2 in the small intestine (Extended Data Fig. 4d), we were unable to consistently detect anti-TG2 antibodies in the serum (Extended Data Fig. 4e). This may reflect the absence of a mouse homologue of the human VH5-51 gene segment that recognizes TG2 in its germline configuration<sup>14</sup>. The presence of circulating anti-gliadin IgG2c antibodies (Fig. 1d) was indicative of gliadin-specific activation of B cells by anti-gluten T<sub>H</sub>1 T cells. In accordance, IFN $\gamma$ —the predominant cytokine associated with coeliac disease in humans<sup>15</sup>—was upregulated in the lamina propria of gluten-fed DQ8-D<sup>d</sup>-villin-IL-15tg mice (Fig. 1e).

Studies in humans suggest that the expansion of IELs that express the activating natural killer receptor NKG2D and the heterodimer formed by NKG2C and CD94 (NKG2C-CD94) in the absence of inhibitory NKG2A-CD94<sup>16,17</sup> mediate cytotoxicity of IECs. IECs destruction is facilitated via the recognition of non-classical MHC molecules MICA, MICB and HLA-E, which are induced after stress and are the main ligands for NKG2D and NKG2C, respectively<sup>16–18</sup>. In accordance with the selective development of villous atrophy in gluten-fed mice overexpressing IL-15 both in the lamina propria and IECs, analysis of IELs revealed that only DQ8-D<sup>d</sup>-villin-IL-15tg mice displayed expansion of degranulating IE-CTLs with a fully activated killer phenotype, as assessed by activating natural killer receptors, granzyme B and perforin expression (Extended Data Fig. 3e–j). Acquisition of cytotoxic features by IELs was gluten-dependent (Extended Data Fig. 4f–l) and accompanied by the upregulation of RAE-1, the mouse ligand for NKG2D (Fig. 1f, Extended Data Figs. 1f, 3k) and QA-1, the mouse ligand for NKG2 receptors paired with CD94 (Fig. 1g, Extended Data Fig. 1g) in the epithelium. Finally, supporting the notion that IE-CTLs are the key effector cells that mediate

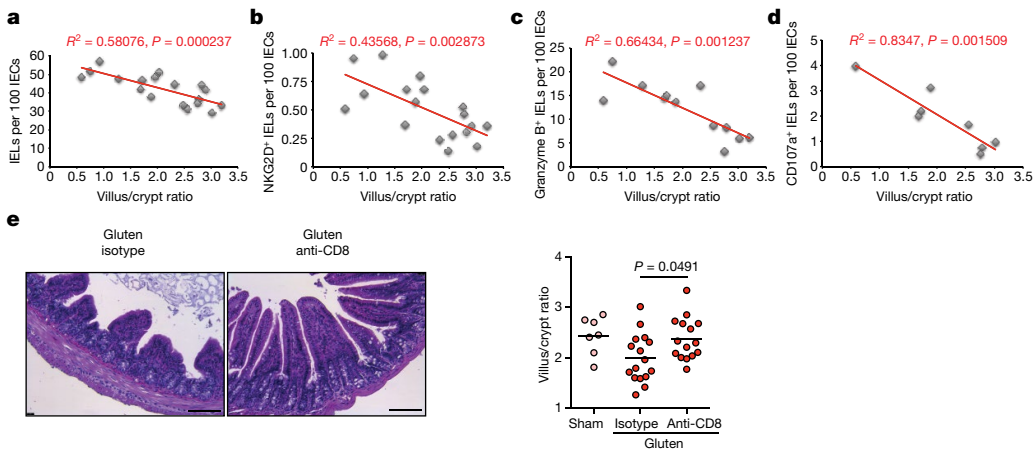


**Fig. 2 | Cytotoxic IELs are the key effector cells that mediate tissue destruction.** **a–d**, Correlations between the extent of villous atrophy determined by analysis of the villus/crypt ratio (Extended Data Fig. 1e) and the number of IELs per 100 IECs (Extended Data Fig. 1d) (a), the number of IELs that express NKG2D per 100 IECs (Extended Data Fig. 2b) (b), the number of IELs that express granzyme B per 100 IECs (Extended Data Fig. 2f) (c), and the number of IELs that express CD107a per 100 IECs (Extended Data Fig. 2i) (d) in sham and gluten-fed DQ8-D<sup>d</sup>-villin-IL-15tg mice. **e**, Left, H&E staining of ileum

sections of DQ8-D<sup>d</sup>-villin-IL-15tg mice fed gluten for 30 days and concurrently treated with a CD8-depleting antibody or an isotype control (treatment regimen and efficacy summarized in Extended Data Fig. 5). Scale bar, 100  $\mu$ m. Right, the villus/crypt ratio (sham,  $n=7$ ; gluten  $n=16$ ; gluten + anti-CD8,  $n=15$ ). Data are from three (a, b) or two (c, d) independent experiments. Data in e are mean values from four independent experiments.  $P$  values determined by Pearson's correlation test (a–d) or one-way ANOVA with Tukey's multiple comparison (e).

tissue destruction in coeliac disease, the number of IE-CTLs with cytolytic functions was correlated with the development of villous atrophy (Fig. 2a–d), and depletion of CD8<sup>+</sup> IE-CTLs in gluten-fed DQ8-D<sup>d</sup>-villin-IL-15tg mice was associated with a conservation of intestinal morphology (Fig. 2e, Extended Data Fig. 5). Together, these data demonstrate that the overexpression of IL-15 in IECs and in the lamina propria need to synergize to activate IE-CTLs. These findings provide a mechanistic basis for why potential patients with coeliac disease with adaptive anti-gluten immunity and family members with IL-15 overexpression in IECs lack IE-CTLs with a fully activated phenotype and do not develop villous atrophy. Despite the high prevalence of HLA-DQ8 in the general population (up to 40% in certain populations), only 1% of individuals develop coeliac disease<sup>1</sup>. In agreement with such observations, HLA-DQ8 transgenic mice did not acquire IE-CTLs with a fully activated killer phenotype (Extended Data Fig. 3e–j) and hence did not develop villous atrophy after gluten feeding (Extended Data Fig. 3a).

Coeliac disease is characterized by the presence of HLA-DQ2- or HLA-DQ8-restricted gluten-specific T cells that produce IFN $\gamma$  and IL-21 in the lamina propria<sup>4</sup>. An analysis of D<sup>d</sup>-villin-IL-15tg mice that lack these HLA molecules but express I-A<sup>b</sup> MHC class II molecules revealed that HLA-DQ8 is not required for the development of the T<sub>H</sub>1 anti-gluten response (Extended Data Fig. 6a–c), even though it is crucial for the development of villous atrophy (Fig. 3a). Consistent with the vital role of HLA-DQ8 in the destruction of IECs, gluten-fed DQ8-D<sup>d</sup>-villin-IL-15tg mice in which CD4<sup>+</sup> T cells were depleted also did not develop villous atrophy (Fig. 3c). Analysis of IE-CTLs in mice lacking HLA-DQ8 or CD4<sup>+</sup> T cells suggested that HLA-DQ8 and CD4<sup>+</sup> T cells are crucial in promoting the licensing of IE-CTLs to kill IECs in DQ8-D<sup>d</sup>-villin-IL-15tg mice fed gluten (Fig. 3a–d, Extended Data Figs. 6d–f, 7a–f). In addition, depletion of CD4<sup>+</sup> T cells suggested that CD4<sup>+</sup> T cells have a role in the upregulation of RAE-1 (Extended Data Fig. 7g) but not QA-1 (Extended Data Fig. 7h), and were required for the generation of anti-DGP and anti-gliadin IgG2c antibodies (Extended Data Fig. 7i–l). These findings uncover a potential mechanistic basis for the role of CD4<sup>+</sup> T cells in the pathogenesis of coeliac disease and why the disease only develops in individuals with HLA-DQ2 or HLA-DQ8.

To further decipher the role of HLA-DQ8, we conducted a comparative transcriptional analysis of total cells isolated from the epithelium of gluten-fed DQ8, D<sup>d</sup>-villin-IL-15tg and DQ8-D<sup>d</sup>-villin-IL-15tg mice. This

analysis revealed that the interplay between HLA-DQ8, IL-15 and gluten was crucial to enable transcriptional pathways in the epithelium and the lamina propria downstream of IFN $\gamma$  (Fig. 3e, f, Extended Data Fig. 8a, b). Furthermore, a large number of pathways related to lymphocyte activation and antigen presentation were enriched in gluten-fed DQ8-D<sup>d</sup>-villin-IL-15tg mice as compared to D<sup>d</sup>-villin-IL-15tg or DQ8 mice in both the lamina propria and the epithelium (Extended Data Fig. 8c, d and Supplementary Dataset 1 for the entire list of Gene Ontology terms enriched in all strains among genes responding to gluten challenge). The finding that HLA-DQ8 was critical for the IFN $\gamma$  response, combined with the observation that gluten-specific T cells in patients with coeliac disease produce IL-21 in addition to IFN $\gamma$ <sup>19</sup>, led us to evaluate the direct contribution of IFN $\gamma$  and IL-21 to disease pathogenesis using neutralizing antibodies. Notably, IFN $\gamma$  (Fig. 3g, h), but not IL-21 (Extended Data Fig. 9a, b), was required for the development of villous atrophy and expansion of IELs. In addition, IFN $\gamma$  alone (Fig. 3i) or in combination with IL-21 promotes the expansion of granzyme B<sup>+</sup> IE-CTLs (Extended Data Fig. 9c–e). Finally, IFN $\gamma$  and IL-21 may have a cooperative role in the generation of anti-DGP and anti-gliadin IgG2c antibodies, as only concomitant neutralization of both cytokines significantly decreased the levels of these anti-gliadin antibodies (Fig. 3j, k, Extended Data Fig. 9f–i). Together, our results demonstrate that IFN $\gamma$  is crucial for the development of villous atrophy, and indicate that IL-15 in the lamina propria has a role in the induction of T<sub>H</sub>1 immunity, whereas HLA-DQ8 promotes and amplifies pathways downstream of IFN $\gamma$ .

TG2 increases the affinity of gluten peptides for HLA-DQ2 and HLA-DQ8 by deamidating specific Gln residues in these peptides to Glu<sup>4,20,21</sup>. We first established that TG2 in the small intestine is activated and that two different pharmacological inhibitors of TG2 (ERW1041E and CK805)<sup>22</sup> were able to inhibit its activity in vivo, as assessed by incorporation of the TG2 activity probe 5-BP into intestinal tissue, and a reduction in antibodies against DGP but not native gliadin peptides (Fig. 4a, Extended Data Fig. 10a). Consistent with the concept that TG2 has a crucial role in the pathogenesis of coeliac disease by amplifying the anti-gluten T cell response in the context of HLA-DQ2 or HLA-DQ8 molecules, the administration of the TG2 inhibitors ERW1041E and CK805 with dietary gluten prevented the development of villous atrophy (Fig. 4b). Together, our findings suggest that TG2 constitutes a therapeutic target for the treatment of coeliac disease, and indicate that

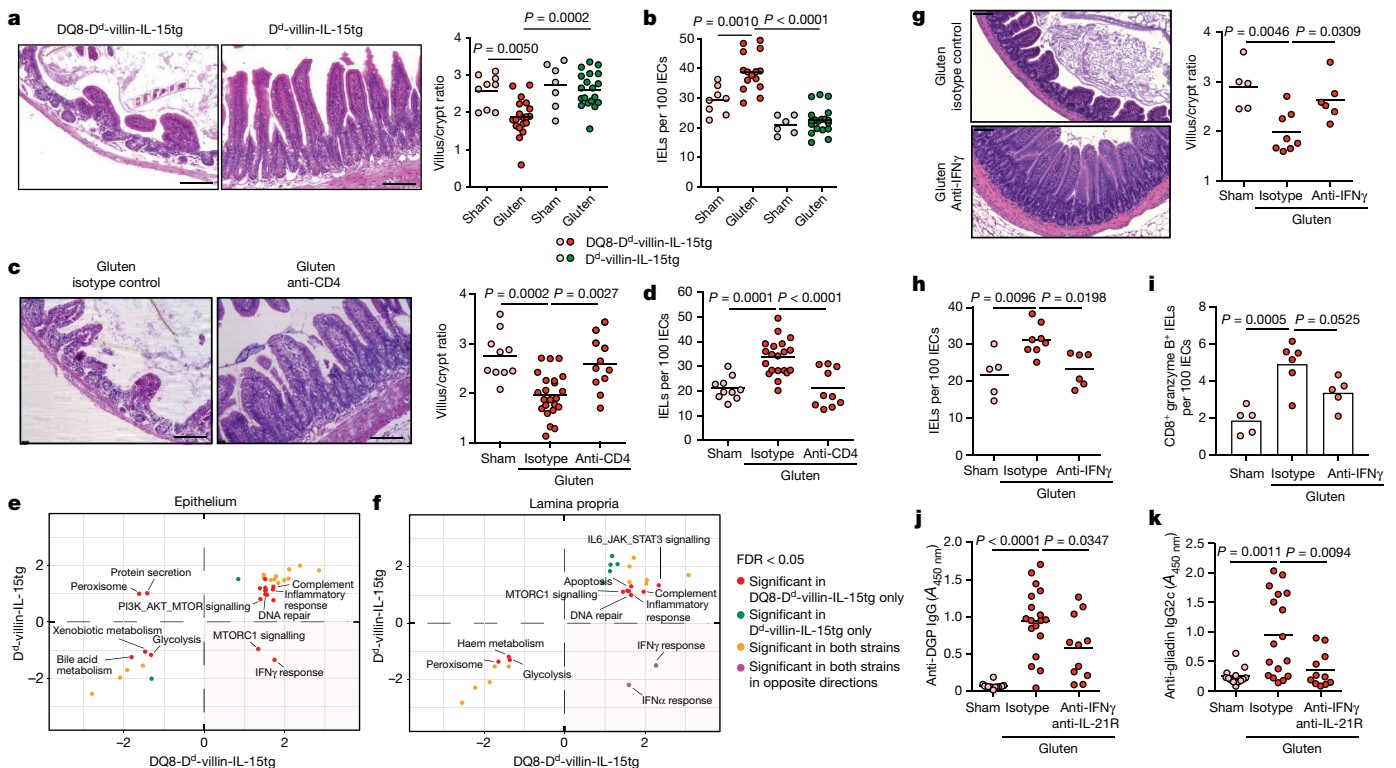


**Fig. 3 | HLA-DQ8, CD4<sup>+</sup> T cells and IFN $\gamma$  are required for tissue destruction.**

**a, b,** DQ8-D<sup>d</sup>-villin-IL-15tg and D<sup>d</sup>-villin-IL-15tg mice were maintained on a GFD or fed gluten for 30 days. **a**, Left, H&E staining of paraffin-embedded ileum sections of gluten-fed mice. Scale bars, 100  $\mu$ m. Right, the villus/crypt ratio (DQ8-D<sup>d</sup>-villin-IL-15tg, sham  $n$  = 9, gluten  $n$  = 19; D<sup>d</sup>-villin-IL-15tg, sham  $n$  = 7, gluten  $n$  = 19). **b**, Quantification of IELs among IECs (DQ8-D<sup>d</sup>-villin-IL-15tg, sham  $n$  = 8, gluten  $n$  = 15; D<sup>d</sup>-villin-IL-15tg, sham  $n$  = 6, gluten  $n$  = 19). **c, d**, DQ8-D<sup>d</sup>-villin-IL-15tg mice were maintained on a GFD, fed gluten for 30 days or fed gluten and concurrently treated with an anti-CD4 antibody (treatment regimen and efficacy summarized in Extended Data Fig. 7). **c**, Left, H&E staining of ileum sections. Scale bars, 100  $\mu$ m. Right, the villus/crypt ratio (sham,  $n$  = 10; gluten  $n$  = 23; gluten + anti-CD4,  $n$  = 11). **d**, Quantification of IELs among IECs (sham,  $n$  = 10; gluten  $n$  = 20; gluten + anti-CD4,  $n$  = 10). **e, f**, Gene set enrichment analysis for gluten-responsive genes in DQ8-D<sup>d</sup>-villin-IL-15tg and D<sup>d</sup>-villin-IL-15tg mice. We contrast the enrichment scores for DQ8-D<sup>d</sup>-villin-IL-15tg ( $x$  axis) and D<sup>d</sup>-villin-IL-15tg mice ( $y$  axis) for all pathways enriched at a false discovery rate (FDR) < 5% in at least one of the strains, in the epithelium and the lamina propria. Positive and negative scores represent enrichments among genes that are more highly and lowly expressed in gluten-fed mice, respectively. Bottom

right quadrant refers to pathways, notably IFN $\gamma$ , that in response to gluten are upregulated in DQ8-D<sup>d</sup>-villin-IL-15tg but downregulated in D<sup>d</sup>-villin-IL-15tg mice. IFN $\gamma$  shows a reversed response to gluten when comparing DQ8-D<sup>d</sup>-villin-IL-15tg with DQ8 mice (Extended Data Fig. 8). **g–k**, DQ8-D<sup>d</sup>-villin-IL-15tg mice were maintained on a GFD, fed gluten for 30 days and concurrently treated with anti-IFN $\gamma$  antibody, anti-IFN $\gamma$  plus IL-21R antibodies together, or isotype control. **g**, Left, H&E staining of ileum sections. Scale bars, 100  $\mu$ m. Right, the villus/crypt ratio (sham,  $n$  = 5, gluten  $n$  = 8, gluten + anti-IFN $\gamma$ ,  $n$  = 6). **h**, Quantification of IELs among IECs (sham,  $n$  = 5; gluten  $n$  = 8; gluten + anti-IFN $\gamma$ ,  $n$  = 6). **i**, The intestinal epithelium was isolated and analysed by flow cytometry. IELs were identified as TCR $\beta$ <sup>+</sup>CD4<sup>+</sup>CD8<sup>+</sup> cells. Granzyme B<sup>+</sup> IELs are indicated by absolute number per 100 IECs (sham,  $n$  = 5, gluten + isotype,  $n$  = 6, gluten + anti-IFN $\gamma$ ,  $n$  = 5). **j**, Serum anti-DGP IgG levels were measured by ELISA 30 days after gluten feeding (sham,  $n$  = 14; gluten  $n$  = 18; gluten + anti-IFN $\gamma$  + anti-IL-21R,  $n$  = 11). **k**, Serum anti-gliadin IgG2c levels (sham,  $n$  = 13; gluten  $n$  = 17; gluten + anti-IFN $\gamma$  + anti-IL-21R,  $n$  = 11). Data are mean values from six (**a–d**), four (**j, k**) or two (**g–i**) experiments. All  $P$  values were determined by ANOVA with Tukey's multiple comparison.

DQ8-D<sup>d</sup>-villin-IL-15tg mice represent a relevant animal model for drug development and discovery. Finally, the value and relevance of DQ8-D<sup>d</sup>-villin-IL-15tg mice as a preclinical model for coeliac disease was further supported by observations that differences in gene expression between gluten-fed DQ8 and DQ8-D<sup>d</sup>-villin-IL-15tg mice were strongly correlated with the changes in gene expression observed between patients with active coeliac disease and healthy controls (Fig. 4c,  $P < 1 \times 10^{-5}$  for both the epithelium and the lamina propria). Furthermore, there was a strong concordance between the Gene Ontology terms enriched among genes induced by gluten challenge in DQ8-D<sup>d</sup>-villin-IL-15tg mice and genes that were differentially expressed between patients with active coeliac disease and healthy controls (Extended Data Fig. 10b, c).

## Discussion

Our study presents the first, to our knowledge, pathophysiological mouse model of coeliac disease in which the ingestion of gluten in an immunocompetent host is enough to promote small intestinal villous

atrophy in a gluten- and HLA-DQ8-dependent manner—the same features seen in patients with active coeliac disease.

Complex immune disorders such as coeliac disease do not develop from the functional defect of a single gene, but instead from the cumulative effect of small changes in gene expression across many immune-relevant genes. Our study suggests that IL-15, HLA-DQ8, TG2, CD4<sup>+</sup> T cells, IE-CTLs and gluten cooperatively regulate disease immunopathology to promote villous atrophy by up-regulating the IFN $\gamma$  response and promoting the expansion of IE-CTLs with a fully activated cytolytic phenotype (Extended Data Fig. 11). The absence of crucial checkpoints in previous mouse models using either lymphopenic mice that lack regulatory T cells<sup>23</sup> or T cell receptor transgenic mice with a high frequency of dietary-antigen specific T cells<sup>12</sup> may explain why villous atrophy developed in these mice in absence of the disease-predisposing HLA molecules DQ2 or DQ8. Together, our findings demonstrate how coeliac disease develops as the result of a complex interaction between several innate and adaptive immune pathways that culminates in tissue destruction, and provide a mechanistic basis for the wide spectrum of clinical

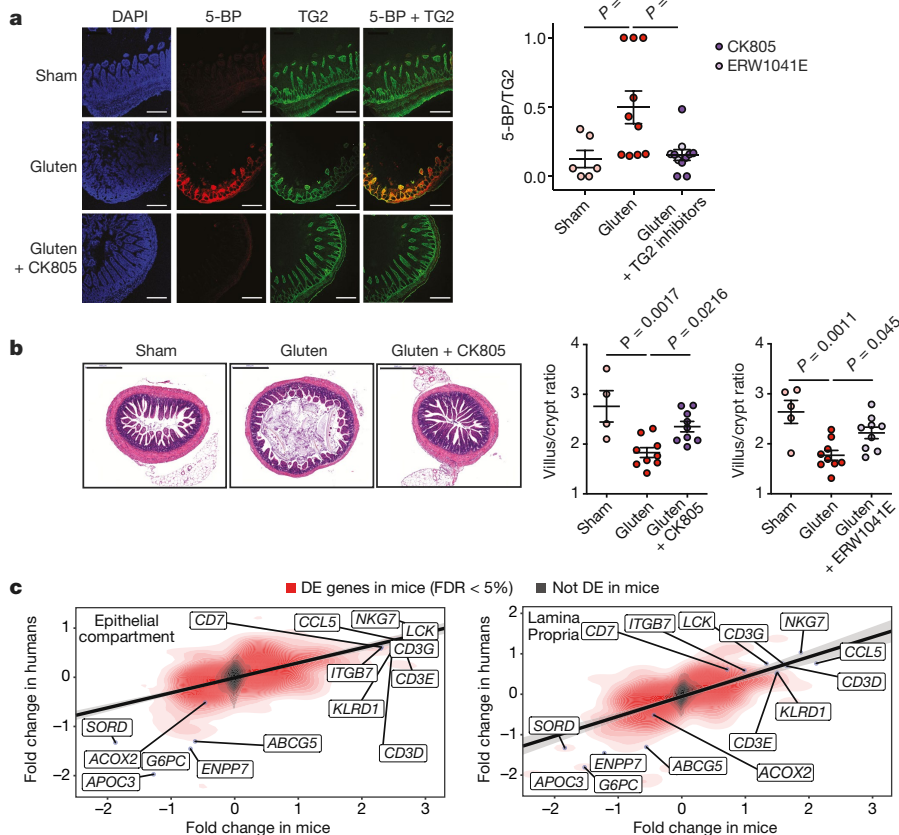


**Fig. 4 | DQ8-D<sup>d</sup>-villin-IL-15tg mice represent a preclinical model for coeliac disease.** **a–b**, DQ8-D<sup>d</sup>-villin-IL-15tg mice were maintained on a GFD, fed gluten for 30 days, or fed gluten and concurrently treated with TG2 inhibitors ERW1041E or CK805 twice a day (25 mg kg<sup>-1</sup> intraperitoneally) for 30 days.

**a**, Left, TG2 protein (green) and enzymatic activity (red, as assessed by crosslinking of 5-biotinamido pentylamine (5-BP)) were distinguished by immunohistochemistry staining of frozen ileum sections. Scale bars, 200 μm. Right, semi-quantitative analysis of the intensity of TG2 activity (5-BP) relative to total TG2 protein; each point represents relative TG2 activity of an individual mouse (sham,  $n=6$ ; gluten,  $n=10$ ; gluten + TG2 inhibitors,  $n=11$ ). **b**, Left, H&E staining of paraffin-embedded ileum sections. Scale bars, 200 μm. Right, the villus/crypt ratio (left graph: sham,  $n=4$ ; gluten,  $n=9$ ; gluten + CK805,  $n=9$ ; right graph: sham,  $n=5$ ; gluten,  $n=9$ ; gluten + ERW1041E,  $n=9$ ). **c**, Transcriptional correlation between the log<sub>2</sub>-transformed fold changes in gene expression between gluten-fed DQ8 and DQ8-D<sup>d</sup>-villin-IL-15tg mice (*x* axis) in the epithelial compartment (that encompass IELs and IECs) (left) or the lamina propria (right) and the log<sub>2</sub>-transformed fold changes in gene expression observed in whole biopsies from patients with active coeliac disease ( $n=51$ ) as compared to healthy controls ( $n=45$ ) (y axis). The red density gradient shows the correlation among genes that are differentially expressed (DE) in gluten-fed DQ8-D<sup>d</sup>-villin-IL-15tg mice. *P* values determined by one-way ANOVA with Tukey's multiple comparison (**a**, **b**). Data in **a** and **b** are mean ± s.e.m. from three (**a**) or two (**b**) independent experiments.

presentation of the disease<sup>5</sup>. By recapitulating key immunological and transcriptional aspects and requirements of coeliac disease, the DQ8-D<sup>d</sup>-villin-IL-15tg transgenic mouse model offers a unique opportunity for preclinical validation of new therapeutic strategies.

## Online content

Any methods, additional references, Nature Research reporting summaries, source data, extended data, supplementary information, acknowledgements, peer review information; details of author contributions and competing interests; and statements of data and code availability are available at <https://doi.org/10.1038/s41586-020-2003-8>.

- Abadie, V., Sollid, L. M., Barreiro, L. B. & Jabri, B. Integration of genetic and immunological insights into a model of celiac disease pathogenesis. *Annu. Rev. Immunol.* **29**, 493–525 (2011).
- Green, P. H. & Cellier, C. Celiac disease. *N. Engl. J. Med.* **357**, 1731–1743 (2007).
- Plugis, N. M. & Khosla, C. Therapeutic approaches for celiac disease. *Best Pract. Res. Clin. Gastroenterol.* **29**, 503–521 (2015).
- Jabri, B. & Sololid, L. M. Tissue-mediated control of immunopathology in coeliac disease. *Nat. Rev. Immunol.* **9**, 858–870 (2009).
- Husby, S. et al. European Society for Pediatric Gastroenterology, Hepatology, and Nutrition guidelines for the diagnosis of coeliac disease. *J. Pediatr. Gastroenterol. Nutr.* **54**, 136–160 (2012).
- Dieterich, W. et al. Identification of tissue transglutaminase as the autoantigen of celiac disease. *Nat. Med.* **3**, 797–801 (1997).
- Jabri, B. & Abadie, V. IL-15 functions as a danger signal to regulate tissue-resident T cells and tissue destruction. *Nat. Rev. Immunol.* **15**, 771–783 (2015).
- Waldmann, T. A. The biology of interleukin-2 and interleukin-15: implications for cancer therapy and vaccine design. *Nat. Rev. Immunol.* **6**, 595–601 (2006).
- Setty, M. et al. Distinct and synergistic contributions of epithelial stress and adaptive immunity to functions of intraepithelial killer cells and active celiac disease. *Gastroenterol.* **149**, 681–691 (2015).
- Black, K. E., Murray, J. A. & David, C. S. HLA-DQ determines the response to exogenous wheat proteins: a model of gluten sensitivity in transgenic knockout mice. *J. Immunol.* **169**, 5595–5600 (2002).
- Jabri, B. & Sololid, L. M. Mechanisms of disease: immunopathogenesis of celiac disease. *Nat. Clin. Pract. Gastroenterol. Hepatol.* **3**, 516–525 (2006).
- Korneychuk, N. et al. Interleukin 15 and CD4<sup>+</sup> T cells cooperate to promote small intestinal enteropathy in response to dietary antigen. *Gastroenterology* **146**, 1017–1027 (2014).
- De Paolo, R. W. et al. Co-adjuvant effects of retinoic acid and IL-15 induce inflammatory immunity to dietary antigens. *Nature* **471**, 220–224 (2011).
- Di Niro, R. et al. High abundance of plasma cells secreting transglutaminase 2-specific IgA autoantibodies with limited somatic hypermutation in celiac disease intestinal lesions. *Nat. Med.* **18**, 441–445 (2012).
- Nilsen, E. M. et al. Gluten induces an intestinal cytokine response strongly dominated by interferon gamma in patients with celiac disease. *Gastroenterology* **115**, 551–563 (1998).
- Meresse, B. et al. Reprogramming of CTLs into natural killer-like cells in celiac disease. *J. Exp. Med.* **203**, 1343–1355 (2006).
- Meresse, B. et al. Coordinated induction by IL15 of a TCR-independent NKG2D signaling pathway converts CTL into lymphokine-activated killer cells in celiac disease. *Immunity* **21**, 357–366 (2004).
- Hüe, S. et al. A direct role for NKG2D/MICA interaction in villous atrophy during celiac disease. *Immunity* **21**, 367–377 (2004).
- Bodd, M. et al. HLA-DQ2-restricted gluten-reactive T cells produce IL-21 but not IL-17 or IL-22. *Mucosal Immunol.* **3**, 594–601 (2010).
- van de Wal, Y. et al. Selective deamination by tissue transglutaminase strongly enhances gliadin-specific T cell reactivity. *J. Immunol.* **161**, 1585–1588 (1998).
- Molberg, O. et al. Tissue transglutaminase selectively modifies gliadin peptides that are recognized by gut-derived T cells in celiac disease. *Nat. Med.* **4**, 713–717 (1998).
- Klöck, C., Herrera, Z., Albertelli, M. & Khosla, C. Discovery of potent and specific dihydroisoxazole inhibitors of human transglutaminase 2. *J. Med. Chem.* **57**, 9042–9064 (2014).
- Freitag, T. L. et al. Gliadin-primed CD4<sup>+</sup>CD45RB<sup>low</sup>CD25<sup>+</sup> T cells drive gluten-dependent small intestinal damage after adoptive transfer into lymphopenic mice. *Gut* **58**, 1597–1605 (2009).

**Publisher's note** Springer Nature remains neutral with regard to jurisdictional claims in published maps and institutional affiliations

© The Author(s), under exclusive licence to Springer Nature Limited 2020

## Methods

### Mice

Mice used in these studies are on the C57BL/6 background. Mice were maintained under specific pathogen-free conditions at the University of Chicago and at the Sainte-Justine University Hospital Research Center. Importantly, no differences in the outcome of the experiments were observed between the two institutions, enabling pooling of the data. HLA-DQ8 transgenic mice (DQ8) and D<sup>d</sup>-IL-15tg mice expressing IL-15 under the minimal MHC class I D<sup>d</sup> promoter (DQ8-D<sup>d</sup>-IL-15tg in the present study) were previously described<sup>13</sup>. Of note, D<sup>d</sup>-IL-15tg mice express IL-15 in all compartments, and in particular in the lamina propria and mesenteric lymph nodes, but not in the epithelium. Villin-IL-15tg mice expressing IL-15 under the intestine-specific 9Kb villin promoter of IECs<sup>24,25</sup> were crossed to HLA-DQ8 mice (DQ8-villin-IL-15tg mice in the present study). D<sup>d</sup>-IL-15tg mice were then crossed onto DQ8-villin-IL-15tg mice to obtain the first generation DQ8-D<sup>d</sup>-villin-IL-15tg mice. Next generations were obtained by backcrossing DQ8-D<sup>d</sup>-villin-IL-15tg mice with DQ8-villin-IL-15tg mice. Finally, DQ8-D<sup>d</sup>-villin-IL-15tg mice were crossed to D<sup>d</sup>-IL-15tg or villin-IL-15tg mice to obtain D<sup>d</sup>-villin-IL-15tg mice. All mice expressing HLA-DQ8 also express I-A<sup>b</sup> MHC class II molecules. All strains were maintained on a gluten-free chow (AIN76A, Envigo). For all experiments, mice, both male and female, were used at 10 weeks of age. All experiments were performed in accordance with the Institutional Biosafety Committee and the Institutional Care and Use Committee of the University of Chicago, and with the Canadian Council on Animal Care guidelines and the Institutional Committee for Animal Care in Research of the Sainte-Justine University Hospital Research Center.

### Antibodies and flow cytometry

The following conjugated antibodies were purchased from eBioscience: TCR $\beta$  APC (H57-597), CD8 $\alpha$  APC-eFluor 780 (53-6.7), CD8 $\beta$  PE-Cy5 (eBioH35-17.2), CD314 (NKG2D) PE (CX5), NKG2AB6 PE (16a11), CD94 FITC (18d3), CD11c PE (N418). The following antibodies were purchased from BD Biosciences: CD4 PE-Cy7 (GK1.5), CD4 BV711 (GK1.5), CD103 APC (M290), NKG2A/C/E FITC (20d5), CD3 $\epsilon$  FITC (17A2), CD3 $\epsilon$  BUV737 (17A2), IgA FITC (C10-3), CD16/CD32 (Fc Block) (2.4G2), CD107a FITC (1D4B). HLA-DQ8 PE (HLADQ81), CD11c BV421 (N418), CD3 $\epsilon$  PE/Cy7 (145-2c11), EpCAM PerCP/Cy5.5 (G8.8), F4/80(BM8), NK1.1(PK136) and CD45 Pacific Blue (30-F11) were purchased from Biolegend. Rae1 AF647 (FAB1135R) was purchased from R&D Systems. Granzyme B PE (GB12), I-A<sup>b</sup> FITC (M5/114.15.2), CD8 $\alpha$  APC-eFluor 780 (53-6.70), B220 PE-Cyanine7 (RA3-6B2) and LIVE/DEAD Fixable Violet Dead Cell Stain Kit were purchased from Thermo Fisher Scientific.

For CD107a detection, 2 × 10<sup>5</sup> cells in 100  $\mu$ l of culture medium were cultured in a 96-well round-bottom cell for 3.5 h at 37 °C with 100  $\mu$ l of a working solution containing phorbol myristate acetate (PMA) (20 ng ml<sup>-1</sup>), ionomycin (200 ng ml<sup>-1</sup>), and Golgi Stop, and with 10  $\mu$ l of CD107a (0.1  $\mu$ g). After incubation, the plate was centrifuged at 400 g for 5 min and cells were stained with additional antibodies. Flow cytometry was performed with a BD LSRFortessa II cell analyser (BD Biosciences) or BD FACSCanto II cell analyser (BD Biosciences), and data were analysed using FlowJo software (Treestar).

### Isolation of epithelial, lamina propria and mesenteric lymph node cells

Epithelial cells including IELs and lamina propria cells were isolated as previously described<sup>26</sup> using EDTA-containing calcium-free medium and collagenase VIII, respectively. For the analysis of the natural killer receptors by flow cytometry, cytotoxic molecules on IELs by flow cytometry and qPCR, and for the analysis of IFN $\gamma$  expression in lamina propria cells by qPCR, a cell purification step using 40% Percoll (GE Healthcare) was used to enrich lymphocyte cell populations. In brief, PBS-washed epithelial and lamina propria cells were resuspended in

10 ml 40% Percoll solution then centrifuged for 30 min at 3,000g. After removal of the supernatant, cells were washed in PBS and counted. Mesenteric lymph nodes were dissected, made into a single-cell suspension by mechanical disruption and passed through a 70- $\mu$ m nylon cell strainer (Corning).

### Gluten feeding and depletions

To study the response to dietary gluten, mice were transferred from a GFD to a standard rodent chow at the beginning of each experiment and allowed to consume the gluten-containing chow ad libitum. In addition, supplementary gluten (20 mg crude gliadin (Sigma-Aldrich) or 100  $\mu$ g peptic-tryptic digests of gliadin) was administered via intragastric gavage, every other day for 30 or 60 days, using a 22-gauge round-tipped needle (Cadence Science) except for Extended Data Fig. 3b, in which mice only consumed standard rodent chow. To study the effect of reversion to a GFD, mice were fed gluten for 30 days, then placed on a GFD until the end of the experiment.

In some experiments, DQ8-D<sup>d</sup>-villin-IL-15tg mice were injected intraperitoneally before initiation of gluten feeding and every 4–5 days at the time of feeding and continuing until termination with 200  $\mu$ g or 400  $\mu$ g of anti-CD4 (GK1.5, rat IgG2b), or 200  $\mu$ g anti-CD8 $\alpha$  (2.43.1, rat IgG2b) or corresponding isotype controls obtained from the Fitch Monoclonal Antibody Core Facility at the University of Chicago or purchased from BioXCell. In some experiments, DQ8-D<sup>d</sup>-villin-IL-15tg mice were injected intraperitoneally once before initiation of gluten feeding and every 3 days over the course of feeding with 500  $\mu$ g of IFN $\gamma$  blocking antibody (XMG1.2) and/or an IL-21R blocking antibody (4A9) or corresponding isotype controls purchased from BioXCell.

### Preparation of chymotrypsin-digested gliadin, peptic-tryptic digests of gliadin and DGP

Chymotrypsin-digested gliadin was prepared as previously described<sup>27</sup>. To obtain DGP, chymotrypsin-digested gliadin was dissolved in TBS containing 10 mM CaCl<sub>2</sub> and guinea-pig liver transglutaminase (TG2; Zedira) and incubated for 2 h at 37 °C with continuous shaking. The concentration of DGP was calculated based on the concentration of the chymotrypsin-digested gliadin and the volume added during deamidation. Alternatively, in experiments to measure the effects of TG2 inhibition on anti-native gliadin and anti-DGP responses, chymotrypsin-digested gliadin preparations were first dialysed against 5 mM sodium phosphate, pH 7.4, using dialysis tubing with a molecular mass cut-off of 1 kDa and then lyophilized. To obtain DGP, mouse TG2 produced recombinantly in *Escherichia coli* was incubated with the chymotrypsin-digested gliadin preparations in 100 mM MOPS buffer, pH 7.4, containing 5 mM CaCl<sub>2</sub> at a TG2:gliadin ratio of 1:50 (w/w) for 1 h at 37 °C. TG2 was quenched by boiling for 10 min, and the digests were dialysed against 5 mM sodium phosphate, pH 7.4, and lyophilized as described. DGP concentration was determined by BCA assay. To obtain peptic-tryptic digests of gliadin, gliadin was digested in 0.2 N HCl, pH 1.8, with pepsin (Sigma) for 2 h at 37 °C. Once the pH was adjusted to 8.0, the digest was incubated with purified trypsin for 4 h at 37 °C, and thereafter with Cotazym (lipase from porcine pancreas Type II, Sigma) for 2 h under constant stirring. The concentration of peptic-tryptic digests of gliadin was determined using a BCA assay (Pierce).

### Anti-TG2, anti-gliadin and anti-DGP ELISA

Serum was obtained 30 or 60 days after mice received the first gluten feeding. For anti-gliadin IgG2c, IgG and IgA ELISA, high-binding ELISA 96-well plates (Nunc, Thermo-Scientific) were coated with 50  $\mu$ l of 100  $\mu$ g ml<sup>-1</sup> chymotrypsin-digested gliadin in 100 mM Na<sub>2</sub>HPO<sub>4</sub> overnight at 4 °C. Plates were washed three times with PBS containing 0.05% Tween-20 (PBS-T) and blocked with 200  $\mu$ l of 2% bovine serum albumin (BSA) in PBS-T for 2 h at room temperature. Serum was assessed in duplicate and at two dilutions, typically 1:50 and 1:200. Serum was incubated overnight at 4 °C and plates were washed three times with

# Article

PBS-T. Anti-mouse Ig-horseradish peroxidase (HRP) (Southern Biotech) in blocking buffer was added to plates and incubated for 1 h at room temperature. Plates were washed five times with PBS-T. HRP substrate TMB (Thermo Scientific) (50 µl) was added and the reaction stopped by the addition of 50 µl 2 N H<sub>2</sub>SO<sub>4</sub> (Fluka Analytical). Absorbance was read at 450 nm on a Molecular Devices Versamax tunable microplate reader. For anti-DGP IgG ELISA, deamidated chymotrypsin-digested gliadin was coated onto Immulon-2HB ELISA plates (Thermo Scientific) at a concentration of 100 µg ml<sup>-1</sup> in 0.1 M Na<sub>2</sub>HPO<sub>4</sub> (Sigma Aldrich) and incubated overnight at 4 °C. Blocking buffer of 4% BSA, 0.05% Tween-20 in PBS was used, and sera were diluted at 1:200 with a diluent of 0.1% BSA, 0.05% Tween-20 in PBS. Biotinylated anti-mouse IgG and streptavidin-HRP (Both Jackson Immunoresearch) were used as the detection reagents. TMB (Sigma Aldrich) was used as the substrate and the reaction stopped by the addition of 50 µl 2 N H<sub>2</sub>SO<sub>4</sub> (Fluka Analytical). Plates were then read at 450 nm. Levels of anti-DGP IgG and anti-gliadin IgG, IgG2c, IgA were expressed in absorbance values.

## Histology

H&E staining was performed on 5-µm thick sections of 10% formalin-fixed paraffin-embedded ileum. Slides were analysed using a Leica DM 2500 microscope with a HC PLAN APO 20×/0.7 NA and a HCX PL APO 100×/1.40-0.70 objective or a Leica DMI8 microscope with a HC PL FLUOTARL 20×/0.40 and a HC PL APO 40×/0.75 objective and equipped with the image processing and analysis software LasX (Leica). Analysis was performed blinded by two investigators. The villus height-to-crypt depth ratios were obtained from morphometric measurements of five well-oriented villi. The villus-to-crypt ratio was calculated by dividing the villus height by the corresponding crypt depth. Villus height was measured from the tip to the shoulder of the villus or up to the top of the crypt of Lieberkühn. The crypt depth was measured as the distance from the top of the crypt of Lieberkühn to the deepest level of the crypt. The IEL count was assessed by counting the number of IELs among at least 100 enterocytes. Additional 5-µm sections were processed for immunohistochemical detection of granzyme B. Slides were deparaffinized, rehydrated and washed in PBS. Sections were incubated in citrate buffer (1 M pH 6.0) for 20 min at 68 °C. Then the sections were permeabilized with 0.3% Triton X-100 at room temperature for 30 min. Endogenous peroxidase activity was quenched for 15 min with 2% hydrogen peroxide in PBS. Sections were blocked with normal donkey serum (Vector Laboratories) for 1 h and incubated with polyclonal goat IgG anti-mouse granzyme B (R&D Systems) for 2 h at room temperature. Sections were then washed in PBS, incubated with biotinylated anti-goat IgG (Vector Laboratories) for 1 h at room temperature, and stained using the avidin-biotin complex method (Vectastain ABC kit; Vector Laboratories). Colour was developed using 3,3'-diaminobenzidine (Dako Diagnostics) containing hydrogen peroxide. Slides were counterstained with Harris-modified haematoxylin, dehydrated, cleared, mounted and examined under light microscopy as described above.

## Immunohistochemistry

Mice were euthanized and intestines were resected. Distal ileum pieces were snap-frozen in optimum cutting temperature (OCT) compound (Tissue-Tek) submerged in isopentane cooled with liquid nitrogen. Frozen tissues were cryosectioned (5-µm thickness) and sections were fixed for 10 min in acetone. Slides were sequentially rehydrated for 10 min in PBS, treated for 30 min at room temperature with PBS containing 3% bovine serum albumin (BSA), and incubated for 1 h at room temperature with Alexa Fluor 594 anti-mouse CD3 (17A2, rat IgG2b, Biolegend), purified anti-mouse CD138 (281-2, rat IgG2a, BD Biosciences), anti-mouse IgA-biotin (goat IgG, Southern Biotech), or anti-TG2 (rabbit polyclonal, produced by Pacific Immunology as described before<sup>3</sup>) diluted in PBS containing 1% BSA. After three washes in PBS, slides were then incubated for 1 h at room temperature with secondary antibody goat anti-rat IgG Alexa Fluor 488, goat anti-rat IgG Alexa

Fluor 633, Alexa Fluor 594 streptavidin, or goat anti-rabbit Alexa Fluor 488 (Molecular Probes). For IgA staining, slides were blocked for 1 h at room temperature in TBS containing 0.05% Tween-20 (TBS-T) and 3% BSA, and the antibodies were diluted in TBS-T containing 1% BSA. After three washes in PBS, slides were mounted with Fluoromount-G containing DAPI (Southern Biotech).

Plasma cells were quantified on stained frozen sections by counting the number of CD138<sup>+</sup> cells in the small intestinal lamina propria. The small intestinal lamina propria was demarcated by the presence of TG2 protein staining<sup>3,27</sup>, and the number of plasma cells was normalized to the total area measured on a per mouse basis. Counting was performed on at least five villi per mouse.

## Quantification of IELs with cytotoxic properties

Flow cytometry staining of CD45 was used to identify all lymphocyte subsets (excluding the epithelial cells). We next determined the amount of TCRαβ<sup>+</sup> among CD45<sup>+</sup> cells, and the amount of CD8<sup>+</sup> T cells expressing NKG2D among TCRαβ<sup>+</sup> cells—and hence the frequency of CD8<sup>+</sup>NKG2D<sup>+</sup>TCRαβ<sup>+</sup> cells among CD45<sup>+</sup> IELs. On H&E-stained slides, we have determined the total amount of IELs per 100 IECs. We performed the following calculation to approximate the absolute numbers of CD8<sup>+</sup>NKG2D<sup>+</sup> IELs per 100 IECs:

$$((\text{percentage of } \text{CD8}^+ \text{NKG2D}^+ \text{TCR}\alpha\beta^+) \times (\text{number of IELs}/100 \text{ IECs}))/100.$$

## Visualization and quantification of TG2 protein and activity

The biotinylated TG2 substrate 5-BP was synthesized and characterized as previously described<sup>28</sup>. 5-BP was dissolved in PBS, and was administered intraperitoneally (100 mg kg<sup>-1</sup>, two doses) 3 and 6 h before euthanizing, and TG2 protein and activity were quantified via immunohistochemistry according to established protocols<sup>3,27</sup>. The 5-BP/TG2 ratio was determined by averaging signals from at least three images per mouse. To facilitate comparison of data from the three independent experiments, the image with the maximum 5-BP/TG2 ratio from each experiment was assigned a value of one, whereas the image with the minimum 5-BP/TG2 ratio was assigned a value of zero. Values between these ratios were scaled linearly using the minimum–maximum normalization tool in GraphPad Prism 8.0.

## TG2 inhibition

CK805 and ERW1041E were synthesized and characterized as previously described<sup>22</sup>. CK805 was formulated in 40% PBS, 40% PEG-4000 and 20% dimethylsulfoxide (DMSO), and ERW1041E was formulated in 2.5% (2-hydroxypropyl)-β-cyclodextrin, 2.0% Tween-80, 10% DMSO and PBS, as described previously<sup>3</sup>. An initial dose of inhibitor (25 mg kg<sup>-1</sup>, intraperitoneally) was administered 12 h before initiation of gluten feeding, and then every 12 h during the course of the 30-day gluten feeding.

## RNA extraction, cDNA synthesis, and qPCR

Total RNA isolation was performed on epithelial and lamina propria cells using the RNeasy Mini Kit (Qiagen). RNA concentration and quality were determined by UV spectrophotometry (Epoch Microplate Spectrophotometer, BioTek). cDNA synthesis was performed using qScript cDNA SuperMix (QuantaBio) according to the manufacturer's instructions. Expression analysis was performed in technical duplicate via qPCR on an Applied Biosystems StepOne Real-Time PCR Systems (Applied Biosystems) with a Power SYBR Green Master Mix (Thermo Fisher Scientific). Expression levels were quantified and normalized to *Gapdh* expression using the following mouse primer pairs: *Gapdh*: 5'-AGCTCGG TGTGAACGGATTG-3', 5'-TGTAGACCATGTTGAGGTCA-3'; *Ifng*: 5'-ATGAACGCTACACACTGCATC-3', 3'-TCTAGGCTTCAATGACTGT GC-5'; and *Qa1*: 5'-AACACACGGAGTCAGGG-3', 3'-ATCAAGGCCATCA TAGGCCAA-5'. Expression analysis for mouse *Gzmb*, *Prf1* and *Rae1* was performed with TaqMan gene expression assays and normalized to *Gapdh* (Thermo Fisher Scientific). Relative gene expression levels were

determined using the  $\Delta\Delta C_t$  method to calculate the relative changes in gene expression relative to sham-fed mice.

### Gene expression microarray

RNA from mouse samples was obtained as described above, quantified spectrophotometrically, and the quality was assessed with the Agilent 2100 Bioanalyzer (Agilent Technologies). Only samples with no evidence for RNA degradation (RNA integrity number >8) were kept for further experiments. Genome-wide gene expression profiling of the epithelium and lamina propria of five individual DQ8, DQ8-D<sup>d</sup>-villin-IL-15tg, and D<sup>d</sup>-villin-IL-15tg mice were determined by using the MouseWG-6 v2.0 Expression BeadChips from Illumina. Low-level microarray analyses were performed in R, using the Bioconductor software package lumi<sup>29</sup>. We first applied a variance stabilizing transformation to all arrays<sup>30</sup> and then quantile normalized the data. After normalization, we removed probes with intensities indistinguishable from background noise (as measured by the negative controls present on each array).

### Identifying genes differentially expressed between mouse strains

To identify genes differently expressed between the different strains of mice, we used a linear modelling-based approach. Specifically, we used the Bioconductor limma package<sup>31</sup> to fit, for each gene, a linear model with individual treatment (that is, gluten feeding), and mice strains as fixed effects. For each gene, we subsequently used the empirical Bayes approach of Smyth<sup>31</sup> to calculate a moderated *t*-statistic and *P* value. We corrected for multiple testing using the FDR approach of Benjamini and Hochberg<sup>32</sup>.

### Patients

One duodenal biopsy was obtained from 96 individuals undergoing upper gastrointestinal endoscopy during diagnostic work-up at the University of Chicago Medicine and at Mayo Clinic, including 45 healthy controls and 51 untreated patients with active coeliac disease for subsequent RNA sequencing. Control subjects included 29 females and 16 males and underwent upper gastrointestinal endoscopy during a diagnostic work-up for anaemia, failure to thrive or other intestinal disorders not associated with coeliac disease. All controls had normal small intestinal histology, no family history of coeliac disease, and no significant levels of anti-TG2 IgA antibodies in the serum. Patients with active coeliac disease included 31 females and 20 males; all had positive anti-TG2 antibodies and small intestinal enteropathy with increased infiltration of IELs, crypts hyperplasia and villous atrophy, according to currently accepted diagnostic guidelines<sup>5</sup>. Each subject signed an informed consent as provided by the Institutional Review Board of each institution (IRB-12623B for the University of Chicago and IRB-1491-03 for Mayo Clinic).

### RNA sequencing on gut biopsies from healthy controls and patients with coeliac disease

A single duodenal biopsy fragment was directly submerged in RNA-later (QIAGEN), kept at 4 °C for 24 h and then frozen at -80 °C upon RNA later removal until processing. Defrosted tissues were homogenized using magnetic beads and a Cell Tissue Homogenizer (Bullet Blender by Next Advance) and RNA was extracted using RNeasy columns (QIAGEN). RNA integrity was assessed by Bioanalyzer (Agilent). All included samples showed an RNA integrity number (RIN) above 8. RNA-sequencing libraries were prepared using the SMARTer Stranded Total RNA Sample Prep Kit-HI Mammalian by Clontech Laboratories (Takara), according to manufacturer's instructions. Library quality was checked by Bioanalyzer (Agilent) before pooling and sequencing. Indexed cDNA libraries were pooled in equimolar amounts and sequenced with single-end 50-bp reads with a high output Flow Cell (8 lane flow cell) on an Illumina HiSeq4000 at the University of Chicago Genomic Facility.

Adaptor sequences and low-quality score bases (Phred score <20) were first trimmed using Trim Galore (v.0.2.7). The resulting reads were then mapped to the human genome reference sequence (Ensembl GRCh37 release 75) using Kallisto v.0.43.0<sup>33</sup> with a GRCh38 transcript annotation GTF file downloaded from Ensembl rel 87. Gene expression was normalized across samples using the weighted trimmed mean of M-values algorithm (TMM), as implemented in the R package edgeR<sup>34</sup>. After normalization, we log-transformed the data using the voom function in the limma package<sup>35</sup>. For all downstream analyses, we excluded non-coding and lowly expressed genes with a median read count lower than 20 in all samples. Following this pre-processing of the data, we fitted the log-transformed expression estimates to linear models using the lmFit function from the limma package<sup>35</sup> to look at differences in gene expression between controls and patients with coeliac disease, while considering variation in sex and age of the donors. Gene Ontology enrichment analyses were performed in Gorilla<sup>36</sup>. We corrected for multiple testing using the FDR approach of Benjamini and Hochberg<sup>32</sup>.

### Gene set enrichment analyses

Gene set enrichment analyses were run using the javaGSEA Desktop application by the Broad Institute (<http://software.broadinstitute.org/gsea/index.jsp;v.3.0>) against the 'Hallmark gene sets' from the Molecular Signatures Database collection. The gene set enrichment analysis pre-rank mode was used ranking genes according to *t*-statistics for differences in gene expression between sham- and gluten-fed mice (for all three strains separately). The *t*-statistics captures both the significance level and the direction of the effects: large positive and negative values refer to genes showing a significantly higher or low expression in gluten-fed mice as compared to sham-fed mice, respectively. The complete results of these analyses are shown in Supplementary Dataset 2.

### Statistical analysis

Tests were performed as indicated in the figure legends using GraphPad Prism. Data are presented as mean  $\pm$  s.e.m. The statistical test used and *P* values are indicated in each figure legend. *P* < 0.05 was considered to be statistically significant. \**P* < 0.05, \*\**P* < 0.01, \*\*\**P* < 0.001, \*\*\*\**P* < 0.0001. No statistical methods were used to predetermine sample size. The experiments were not randomized, and investigators were not blinded to allocation during experiments and outcome assessment unless stated otherwise.

### Reporting summary

Further information on research design is available in the Nature Research Reporting Summary linked to this paper.

### Data availability

Source Data for Figs. 1–4 and Extended Data Figs. 1–10 are provided with the paper. The RNA sequencing experiments have been deposited into the Gene Expression Omnibus (GEO) database under the accession code GSE134900. All other data are available from the corresponding author(s) upon reasonable request.

24. Meisel, M. et al. Interleukin-15 promotes intestinal dysbiosis with butyrate deficiency associated with increased susceptibility to colitis. *ISME J.* **11**, 15–30 (2017).
25. Pinto, D., Robine, S., Jaïsler, F., El Marjou, F. E. & Louvard, D. Regulatory sequences of the mouse villin gene that efficiently drive transgenic expression in immature and differentiated epithelial cells of small and large intestines. *J. Biol. Chem.* **274**, 6476–6482 (1999).
26. Lefrancois, L. & Lycke, N. Isolation of mouse small intestinal intraepithelial lymphocytes, Peyer's patch, and lamina propria cells. *Curr. Protoc. Immunol.* **Chapter 3**, Unit 3.19 (2001).
27. Bouziat, R. et al. Reovirus infection triggers inflammatory responses to dietary antigens and development of celiac disease. *Science* **356**, 44–50 (2017).
28. DiRaimondo, T. R. et al. Elevated transglutaminase 2 activity is associated with hypoxia-induced experimental pulmonary hypertension in mice. *ACS Chem. Biol.* **9**, 266–275 (2014).
29. Du, P., Kibbe, W. A. & Lin, S. M. lumi: a pipeline for processing Illumina microarray. *Bioinformatics* **24**, 1547–1548 (2008).

# Article

30. Lin, S. M., Du, P., Huber, W. & Kibbe, W. A. Model-based variance-stabilizing transformation for Illumina microarray data. *Nucleic Acids Res.* **36**, e11 (2008).
31. Smyth, G. K. Linear models and empirical bayes methods for assessing differential expression in microarray experiments. *Stat Appl Genet Mol Biol* **3**, Article3 (2004).
32. Benjamini, Y. H. Y. Controlling the false discovery rate: A practical and powerful approach to multiple testing. *J. R. Stat. Soc. Ser. A Stat. Soc.* **57**, 289–300 (1995).
33. Bray, N. L., Pimentel, H., Melsted, P. & Pachter, L. Near-optimal probabilistic RNA-seq quantification. *Nat. Biotechnol.* **34**, 525–527 (2016).
34. Robinson, M. D., McCarthy, D. J. & Smyth, G. K. edgeR: a Bioconductor package for differential expression analysis of digital gene expression data. *Bioinformatics* **26**, 139–140 (2010).
35. Ritchie, M. E. et al. limma powers differential expression analyses for RNA-sequencing and microarray studies. *Nucleic Acids Res.* **43**, e47 (2015).
36. Eden, E., Navon, R., Steinfield, I., Lipsky, D. & Yakhini, Z. GOrilla: a tool for discovery and visualization of enriched GO terms in ranked gene lists. *BMC Bioinformatics* **10**, 48 (2009).

**Acknowledgements** We thank patients with coeliac disease and their family members, as well as the University of Chicago Celiac Disease Center, for supporting our research. We thank BZ-Histo Services for the histological processing of intestinal samples. We also thank the Human Tissue Resource Center and the Integrated Light Microscopy Core Facility at the University of Chicago. This work was supported by grants from NIH: R01 DK67180 and R01 DK63158, and Digestive Diseases Research Core Center P30 DK42086 at the University of Chicago as well as by funding from F. Oliver Nicklin associated with the First Analysis Institute of Integrative Studies and the Regenstein Foundation to B.J., from the CIHR catalyst grant in environments,

genes, and chronic disease) to V.A. and L.B.B., the SickKids Foundation (NI15-040) and the Canadian Celiac Association to V.A., from NIH: R01 DK063158 and R01 DK100619 to C.K., award from the Wallonie-Bruxelles International-World Excellence and from FRQNT to T.L. The Carlino Fellowship for Celiac Disease Research from the University of Chicago Celiac Disease Center supported V.D.

**Author contributions** V.A. and B.J. designed the research and supervised all investigations. S.M.K., T.L., J.D.E., B.A.P., C.C., J.V., R.B., K.P., M.A.Z., A.D., V.Y. and V.A. performed experiments and analysed the data. V.D. and I.L. performed the human RNA sequencing experiments. E.V.M. and I.H. undertook serology experiments. O.T., J.-C.G., M.B.F.H. and L.B.B. performed the computational analysis. C.K., J.A.M. and L.B.B. provided intellectual input and technical support. V.A. and B.J. wrote the manuscript with the contribution of S.M.K., T.L., B.A.P. and C.K. All authors provided critical review of the manuscript.

**Competing interests** B.J. and J.A.M. are consultants to Celimmune and Bionix. C.K. is a member of the Board of Directors of Protagonist Therapeutics. All other authors declare no competing interests.

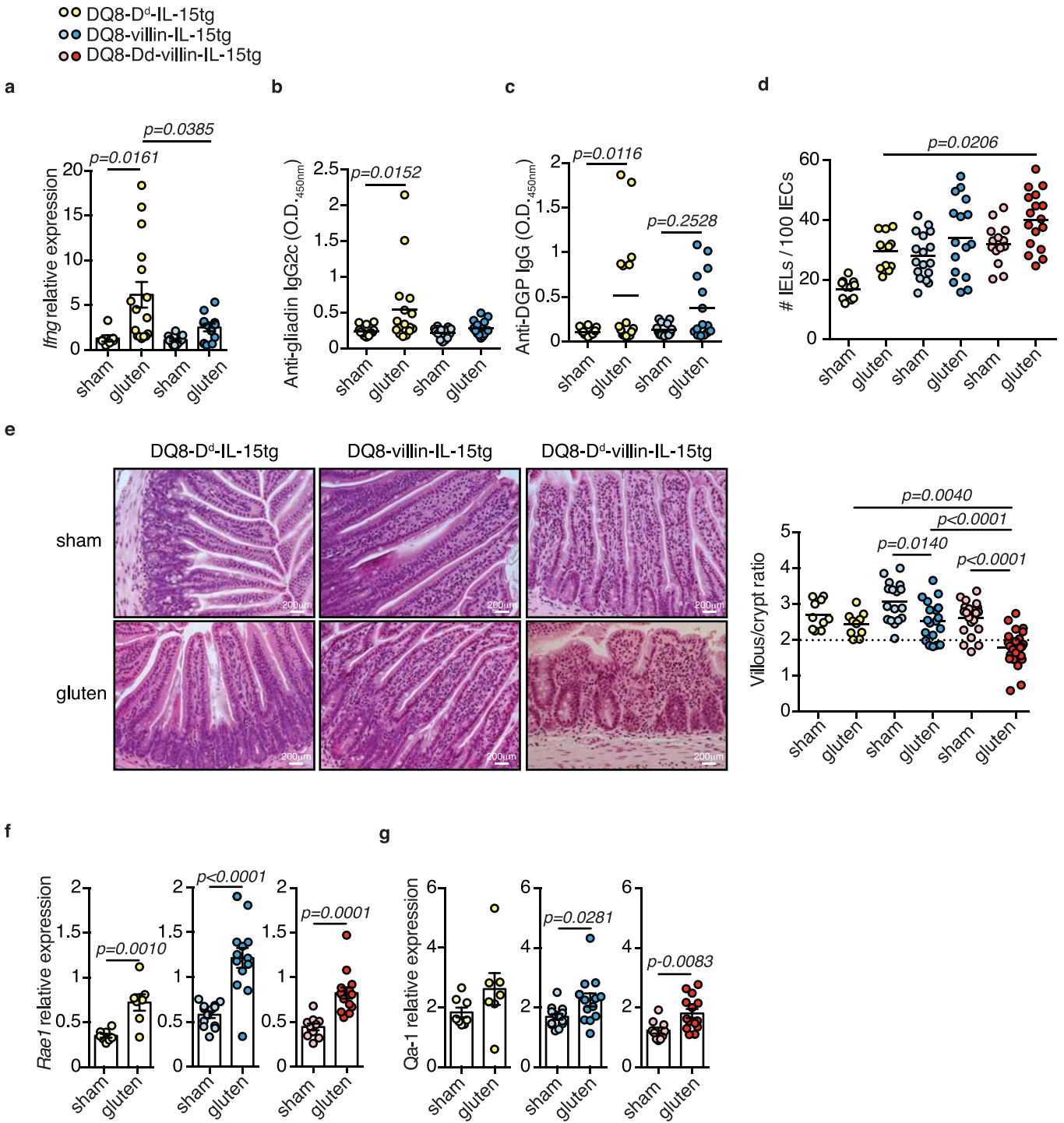
## Additional information

**Supplementary information** is available for this paper at <https://doi.org/10.1038/s41586-020-2003-8>.

**Correspondence and requests for materials** should be addressed to V.A. or B.J.

**Peer review information** *Nature* thanks Nadine Cerf-Bensussan, Arthur Kaser, Daniel Mucida and Emil Unanue for their contribution to the peer review of this work.

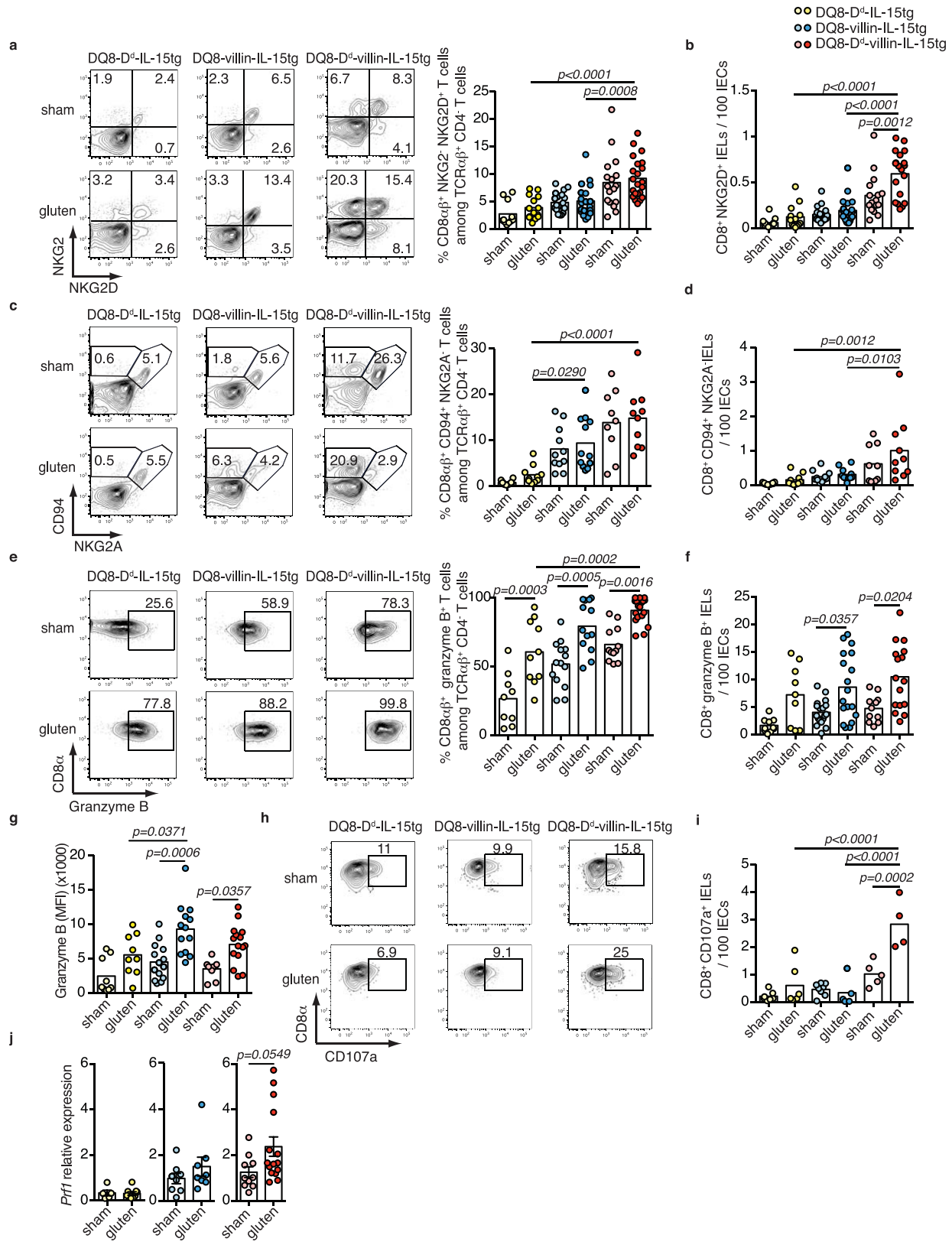
**Reprints and permissions information** is available at <http://www.nature.com/reprints>.



**Extended Data Fig. 1 | Development of villous atrophy requires IL-15 expression in both the lamina propria and epithelium.** **a–g**, DQ8-D<sup>d</sup>-IL-15tg, DQ8-villin-IL-15tg and DQ8-D<sup>d</sup>-villin-IL-15tg mice that were raised on a GFD were maintained on a GFD (sham) or fed gluten for 30 days. **a**, Expression of *Ifng* in the lamina propria was measured by qPCR (DQ8-D<sup>d</sup>-IL-15tg sham, *n* = 7, gluten *n* = 16; DQ8-villin-IL-15tg sham, *n* = 13, gluten *n* = 12). **b**, Serum anti-gliadin IgG2c levels were measured by ELISA 30 days after gluten feeding (DQ8-D<sup>d</sup>-IL-15tg sham, *n* = 16, gluten *n* = 16; DQ8-villin-IL-15tg sham, *n* = 15, gluten *n* = 15). **c**, Serum levels of anti-DGP IgG were measured by ELISA 30 days after gluten feeding (DQ8-D<sup>d</sup>-IL-15tg sham, *n* = 10, gluten *n* = 10; DQ8-villin-IL-15tg sham, *n* = 9, gluten *n* = 9). **d**, Quantification of IELs among IECs was performed on H&E-stained ileum sections (DQ8-D<sup>d</sup>-IL-15tg sham, *n* = 11, gluten *n* = 12; DQ8-villin-IL-

15tg sham, *n* = 17, gluten *n* = 16; DQ8-D<sup>d</sup>-villin-IL-15tg sham, *n* = 14, gluten *n* = 17). **e**, Left, H&E staining of paraffin-embedded ileum sections. Right, the ratio of the morphometric assessment of villus height to crypt depth (DQ8-D<sup>d</sup>-IL-15tg sham, *n* = 10, gluten *n* = 10; DQ8-villin-IL-15tg sham, *n* = 17, gluten *n* = 19; DQ8-D<sup>d</sup>-villin-IL-15tg sham, *n* = 21, gluten *n* = 28). **f,g**, Expression of *Rae1* (**f**) and *Qa1* (**g**) in the intestinal epithelium was measured by qPCR. Relative expression levels in sham and gluten-fed mice for each strain are shown (DQ8-D<sup>d</sup>-IL-15tg sham, *n* = 16, gluten *n* = 16; DQ8-villin-IL-15tg sham, *n* = 15, gluten *n* = 15; DQ8-D<sup>d</sup>-villin-IL-15tg sham, *n* = 20, gluten *n* = 26). Data are mean  $\pm$  s.e.m. (**a,f,g**) or mean values (**b–e**) from three (**a–c,f,g**), four (**d**) or six (**e**) independent experiments. *P* values were determined by one-way ANOVA with Tukey's multiple comparison test (**a–e**) or unpaired, two-tailed, *t*-test (**f,g**).

# Article

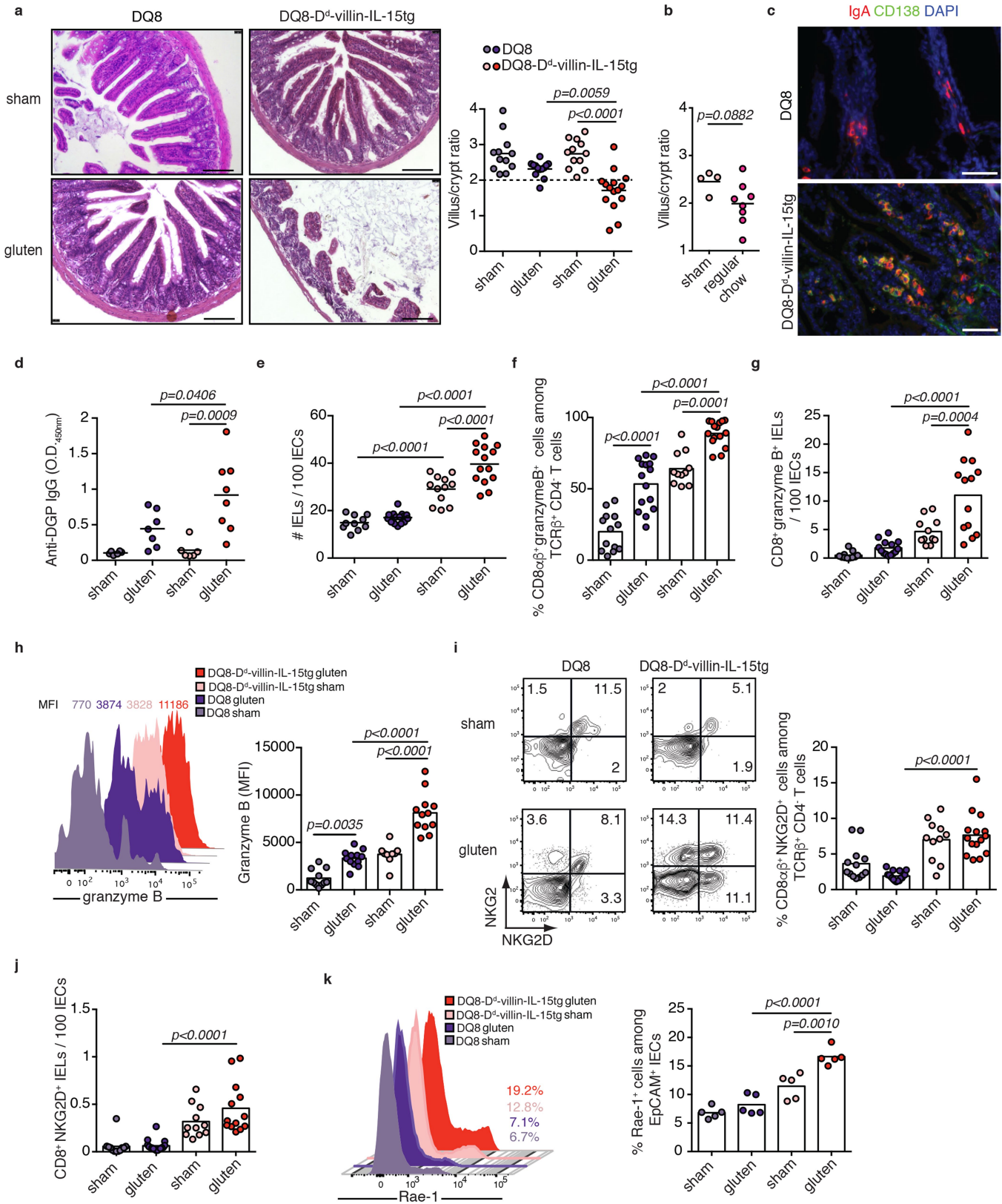


**Extended Data Fig. 2** | See next page for caption.

**Extended Data Fig. 2 | Acquisition of cytotoxic properties by IELs requires IL-15 expression in both the lamina propria and epithelium.** **a–j.** DQ8-D<sup>d</sup>-IL-15tg, DQ8-villin-IL-15tg and DQ8-D<sup>d</sup>-villin-IL-15tg mice were maintained on a GFD or fed gluten for 30 days (gluten). **a–i.** The intestinal epithelium was isolated and analysed by flow cytometry. A subset of IELs was identified as TCR $\beta^+$ CD4 $^-$ CD8 $\alpha\beta^+$  cells. In parallel, IELs were identified as TCR $\beta^+$ CD4 $^-$ CD8 $^+$  cells by flow cytometry and quantified among IECs on H&E-stained ileum sections. **a.** Percentage of NKG2D $^+$ NKG2C $^-$ CD8 $\alpha\beta^+$  IELs are indicated (DQ8-D<sup>d</sup>-IL-15tg sham,  $n=11$ , gluten  $n=14$ ; DQ8-villin-IL-15tg sham,  $n=20$ , gluten  $n=20$ ; DQ8-D<sup>d</sup>-villin-IL-15tg sham,  $n=17$ , gluten  $n=22$ ). **b.** Numbers of NKG2D $^+$ NKG2C $^-$ CD8 $^+$  IELs per 100 IECs (DQ8-D<sup>d</sup>-IL-15tg sham,  $n=11$ , gluten  $n=13$ ; DQ8-villin-IL-15tg sham,  $n=20$ , gluten  $n=20$ ; DQ8-D<sup>d</sup>-villin-IL-15tg sham,  $n=16$ , gluten  $n=19$ ). **c.** Percentage of CD94 $^+$ NKG2A $^-$ CD8 $\alpha\beta^+$  IELs are indicated (DQ8-D<sup>d</sup>-IL-15tg sham,  $n=10$ , gluten  $n=10$ ; DQ8-villin-IL-15tg sham,  $n=11$ , gluten  $n=11$ ; DQ8-D<sup>d</sup>-villin-IL-15tg sham,  $n=9$ , gluten  $n=10$ ). **d.** Numbers of CD94 $^+$ NKG2A $^-$ CD8 $^+$  IELs per 100 IECs (DQ8-D<sup>d</sup>-IL-15tg sham,  $n=10$ , gluten  $n=10$ ; DQ8-villin-IL-15tg sham,  $n=11$ , gluten  $n=11$ ; DQ8-D<sup>d</sup>-villin-IL-15tg sham,  $n=9$ , gluten  $n=10$ ). **e.** Percentage of intracellular granzyme B $^+$  IELs (DQ8-D<sup>d</sup>-IL-

15tg sham,  $n=9$ , gluten  $n=10$ ; DQ8-villin-IL-15tg sham,  $n=14$ , gluten  $n=13$ ; DQ8-D<sup>d</sup>-villin-IL-15tg sham,  $n=12$ , gluten  $n=18$ ). **f.** Numbers of granzyme B $^+$  IELs per 100 IECs (DQ8-D<sup>d</sup>-IL-15tg sham,  $n=11$ , gluten  $n=13$ ; DQ8-villin-IL-15tg sham,  $n=20$ , gluten  $n=20$ ; DQ8-D<sup>d</sup>-villin-IL-15tg sham,  $n=16$ , gluten  $n=19$ ). **g.** Mean fluorescent intensity (MFI) of intracellular granzyme B was measured. (DQ8-D<sup>d</sup>-IL-15tg sham,  $n=9$ , gluten  $n=9$ ; DQ8-villin-IL-15tg sham,  $n=14$ , gluten  $n=13$ ; DQ8-D<sup>d</sup>-villin-IL-15tg sham,  $n=10$ , gluten  $n=15$ ). **h.** Percentage of CD8 $\alpha\beta^+$ CD107a $^+$  IELs. **i.** Numbers of CD8 $^+$ CD107a $^+$  IELs per 100 IECs (DQ8-D<sup>d</sup>-IL-15tg sham,  $n=7$ , gluten  $n=6$ ; DQ8-D<sup>d</sup>-villin-IL-15tg sham,  $n=8$ , gluten  $n=5$ ; DQ8-D<sup>d</sup>-villin-IL-15tg sham,  $n=5$ , gluten  $n=4$ ). **j.** Expression of *Prf1* in the intestinal epithelium was measured by qPCR. Relative expression levels in sham and gluten-fed mice for each strain are shown (DQ8-D<sup>d</sup>-IL-15tg sham,  $n=16$ , gluten  $n=16$ ; DQ8-villin-IL-15tg sham,  $n=15$ , gluten  $n=15$ ; DQ8-D<sup>d</sup>-villin-IL-15tg sham,  $n=20$ , gluten  $n=26$ ). Data are mean  $\pm$  s.e.m. (**j**) or mean values (**a–g, i**) from six (**a, b**), three (**c, d, j**), five (**e, f**), four (**g**) or two (**h, i**) independent experiments. *P* values were determined by one-way ANOVA with Tukey's multiple comparison test (**a–g, i**) or unpaired, two-tailed, *t*-test (**j**).

# Article

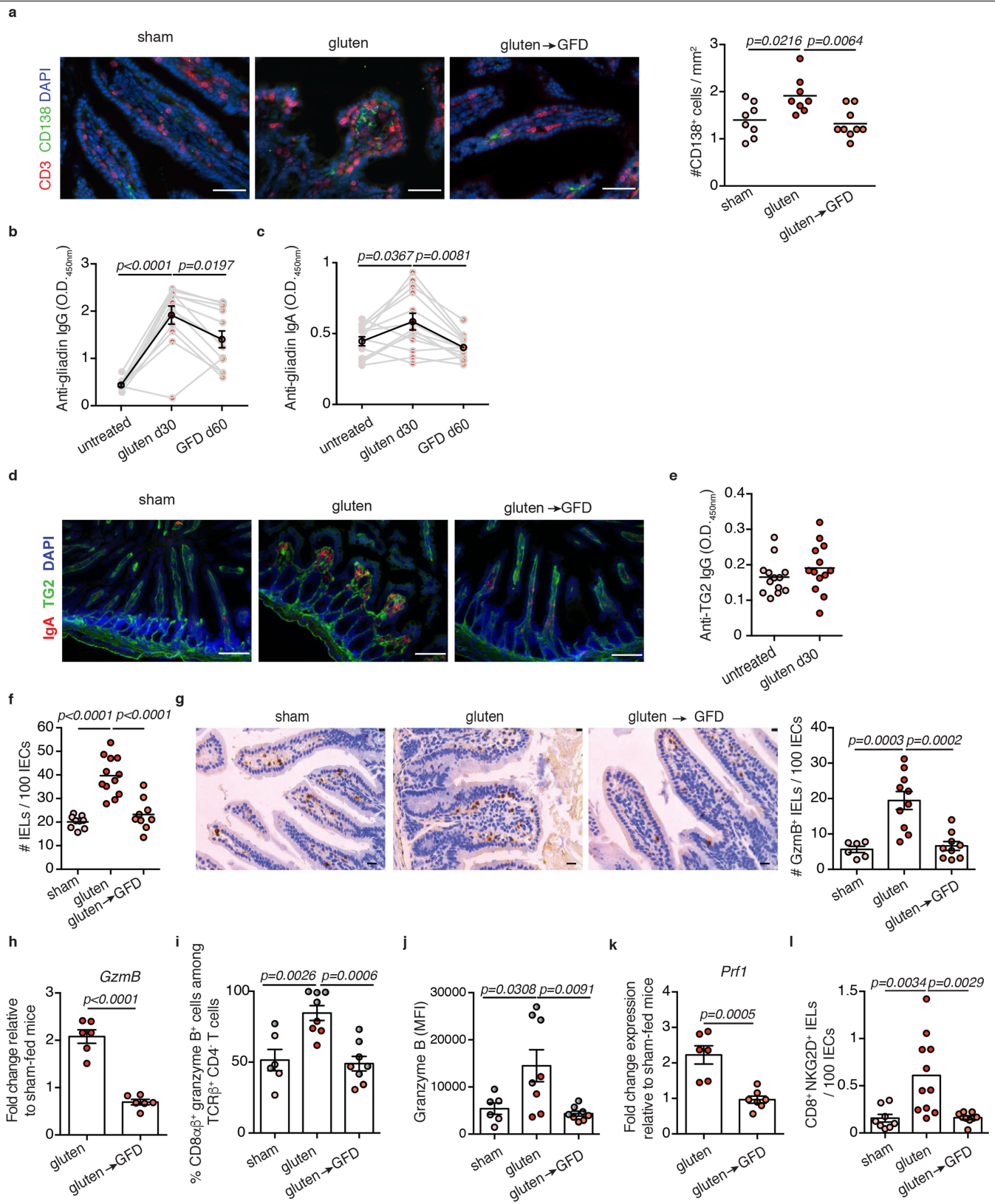


**Extended Data Fig. 3** | See next page for caption.

**Extended Data Fig. 3 | Overexpression of IL-15 in HLA-humanized DQ8 mice confers susceptibility to development of coeliac disease-like features in a gluten-dependent manner.** **a–k**, DQ8 and DQ8-D<sup>d</sup>-villin-IL-15tg mice were maintained on a GFD or fed gluten for 30 days. **a**, Left, H&E staining of paraffin-embedded ileum sections. Scale bars, 100  $\mu$ m. Right, the ratio of the morphometric assessment of villus height to crypt depth (DQ8 sham,  $n=12$ , gluten  $n=13$ ; DQ8-D<sup>d</sup>-villin-IL-15tg sham,  $n=12$ , gluten  $n=15$ ). **b**, Villus/crypt ratio from sham-fed DQ8-D<sup>d</sup>-villin-IL-15tg mice and DQ8-D<sup>d</sup>-villin-IL-15tg mice fed a standard rodent chow without supplementary gluten (sham,  $n=4$ , gluten  $n=8$ ). **c**, IgA (red) and CD138<sup>+</sup> (green) plasma cells were distinguished by immunohistochemical staining of frozen ileum sections. Scale bars, 50  $\mu$ m. **d**, Serum levels of anti-DGP IgG as measured by ELISA. Serum was collected 30 days after gluten feeding (DQ8 sham,  $n=6$ , gluten  $n=7$ ; DQ8-D<sup>d</sup>-villin-IL-15tg sham,  $n=6$ , gluten  $n=7$ ). **e**, Quantification of IELs among IECs performed on H&E-stained ileum sections (DQ8 sham,  $n=10$ , gluten  $n=16$ ; DQ8-D<sup>d</sup>-villin-IL-15tg sham,  $n=12$ , gluten  $n=14$ ). **f–j**, The intestinal epithelium was isolated and

analysed by flow cytometry. IELs were identified as TCR $\beta^+$ CD4 $^-$ CD8 $^+$  and TCR $\beta^+$ CD4 $^-$ CD8 $\alpha\beta^+$  cells. **f**, Percentage of granzyme B<sup>+</sup>IELs (DQ8 sham,  $n=13$ , gluten  $n=15$ ; DQ8-D<sup>d</sup>-villin-IL-15tg sham,  $n=11$ , gluten  $n=15$ ). **g**, Numbers of CD8<sup>+</sup> granzyme B<sup>+</sup>IELs per 100 IECs (DQ8 sham,  $n=11$ , gluten  $n=14$ ; DQ8-D<sup>d</sup>-villin-IL-15tg sham,  $n=11$ , gluten  $n=13$ ). **h**, MFI of granzyme B (DQ8 sham,  $n=11$ , gluten  $n=12$ ; DQ8-D<sup>d</sup>-villin-IL-15tg sham,  $n=9$ , gluten  $n=12$ ). **i**, Percentage of NKG2D $^+$ NKG2 $^-$ IELs (DQ8 sham,  $n=13$ , gluten  $n=17$ ; DQ8-D<sup>d</sup>-villin-IL-15tg sham,  $n=11$ , gluten  $n=15$ ). **j**, Numbers of NKG2D $^+$ NKG2 $^-$ IELs per 100 IECs (DQ8 sham,  $n=12$ , gluten  $n=16$ ; DQ8-D<sup>d</sup>-villin-IL-15tg sham,  $n=11$ , gluten  $n=13$ ). **k**, The intestinal epithelium was isolated and analysed by flow cytometry. IECs were identified as EpCAM $^+$ CD45 $^-$  cells. Percentage of Rae-1 $^+$ IECs ( $n=5$  mice per group). Data are mean values (**a**, **b**, **d–k**) from four (**a**, **e–g**, **i,j**), two (**b**, **d**, **k**) or three (**c**, **h**) independent experiments. *P*values were determined by one-way ANOVA with Tukey's multiple comparison test (**a**, **d–k**) or unpaired, two-tailed, *t*-test (**b**).

# Article

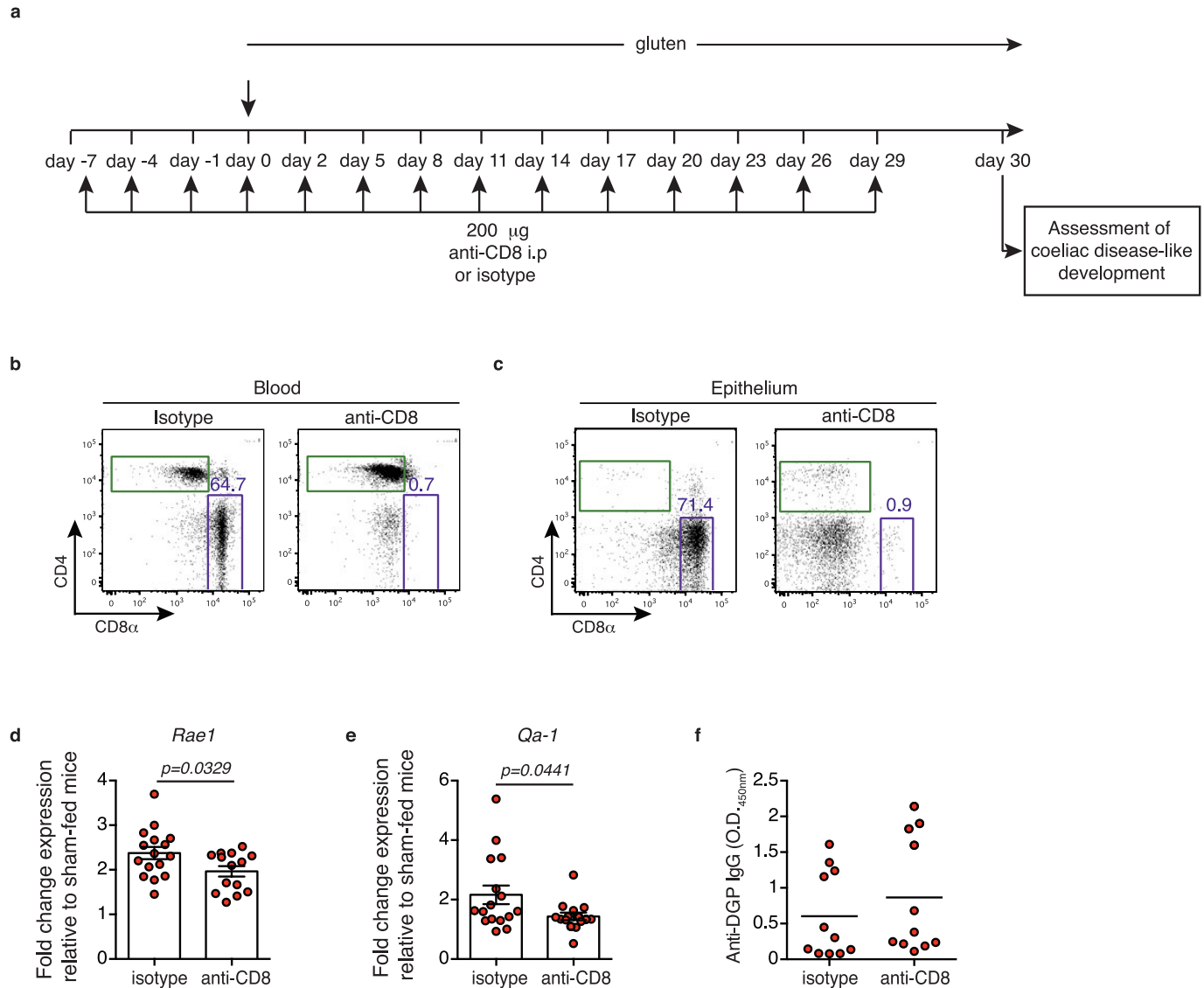


**Extended Data Fig. 4** | See next page for caption.

**Extended Data Fig. 4 | A GFD decreases the anti-gluten antibody response and the number of cytotoxic IELs.** **a–h, k, l**, DQ8-D<sup>d</sup>-villin-IL-15tg mice raised on a GFD were maintained on a GFD, fed gluten for 30 days, or fed gluten for 30 days and then reverted to a GFD for 30 days. **a**, Left, CD3ε<sup>+</sup> T cells (red) and CD138<sup>+</sup> plasma cells (green) were distinguished by immunohistochemistry staining of frozen ileum sections. Scale bars, 50 μm. Right, the number of CD138<sup>+</sup> cells per section, normalized to lamina propria area (sham,  $n=8$  mice; gluten,  $n=8$  mice; gluten→GFD,  $n=9$  mice). **b, c**, Serum levels of anti-gliadin IgG (**b**) and anti-gliadin IgA (**c**) were measured by ELISA. Serum was collected sequentially in the same mice before gluten feeding (untreated), 30 days after gluten feeding (gluten d30), and 30 days after reversion to a GFD (GFD d60) ( $n=12$  or 13 mice per group for anti-gliadin IgG or IgA, respectively). **d**, Mucosal IgA deposits (red) and TG2 (green) were identified by immunohistochemistry staining of frozen ileum sections. Scale bars, 100 μm. **e**, Serum levels of anti-TG2 IgG antibody measured by ELISA 30 days after gluten feeding ( $n=13$  mice per group). **f**, Quantification of IELs among IECs was performed on H&E-stained ileum sections (sham,  $n=8$  mice; gluten,  $n=12$  mice; gluten→GFD,  $n=9$  mice). **g**, Left, granzyme B staining by immunohistochemistry on paraffin-embedded ileum sections. Scale bars, 20 μm. Right, number of granzyme B<sup>+</sup> IELs per 100 IECs per mouse (sham,  $n=6$  mice; gluten,  $n=10$  mice; gluten→GFD,  $n=9$  mice).

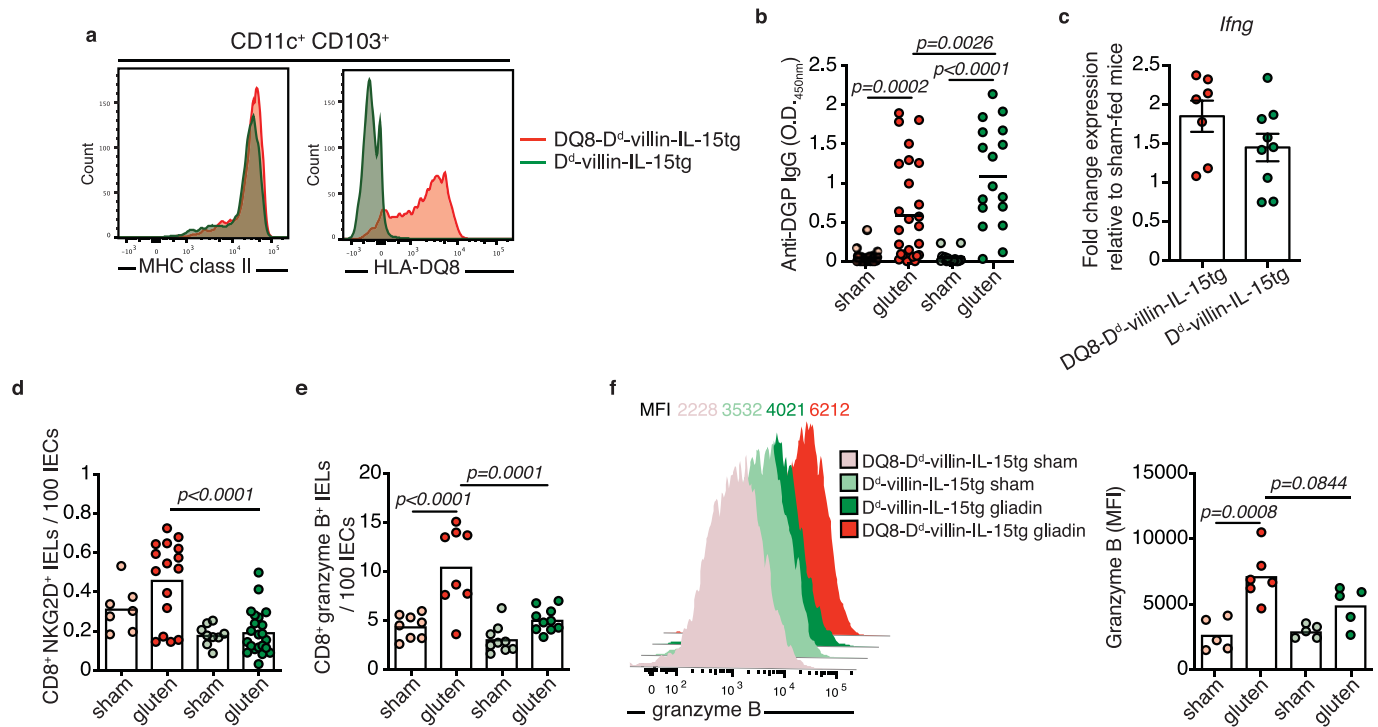
**h**, Expression of *Gzmb* in the intestinal epithelium was measured by qPCR. Relative expression levels in gluten and gluten→GFD groups were normalized against the expression levels observed in sham-fed DQ8-D<sup>d</sup>-villin-IL-15tg mice ( $n=6$  mice per group). **i, j**, DQ8-D<sup>d</sup>-villin-IL-15tg mice raised on a GFD were maintained on a GFD, fed gluten for 30 days, or fed gluten for 30 days and then reverted to a GFD for 60 or 90 days. The intestinal epithelium was isolated and analysed by flow cytometry, and IELs were identified as TCRβ<sup>+</sup>CD4<sup>+</sup>CD8αβ<sup>+</sup> cells. Granzyme B<sup>+</sup> IELs are indicated by percentage (**i**) and MFI (**j**) (sham,  $n=6$  mice; gluten,  $n=8$  mice; gluten→GFD,  $n=8$  mice). **k**, Expression of *Prf1* in the intestinal epithelium was measured by qPCR. Analysis was performed as in **h** (gluten,  $n=6$  mice; gluten→GFD,  $n=7$  mice). **l**, The intestinal epithelium was isolated and analysed by flow cytometry. IELs were identified as TCRβ<sup>+</sup>CD4<sup>+</sup>CD8<sup>+</sup> cells. In parallel, IELs were quantified among IECs on H&E-stained ileum sections. NKG2D<sup>+</sup>NKG2<sup>+</sup> IELs are indicated by absolute number per 100 IECs (sham,  $n=8$  mice; gluten,  $n=11$  mice; gluten→GFD,  $n=9$  mice). Data are mean ± s.e.m. (**b, c, g–l**) or mean values (**a, e, f**) from three (**a, d, g**), four (**b, c, e, f**) or two (**h–l**) independent experiments. *P* values were determined by one-way ANOVA with Tukey's multiple comparison test (**a–c, f, g, i, j, l**) or unpaired, two-tailed, *t*-test (**e, h, k**).

# Article



**Extended Data Fig. 5 | Effect of CD8 $^{+}$  T cell depletion on antibody production and epithelial stress markers.** **a–f**, Ten-week-old DQ8-D $^{d}$ -villin-IL-15tg mice were treated with 200 µg anti-CD8 $\alpha$  antibody (clone 2.43) or its isotype control (rat IgG2b) twice before and during the course of gluten feeding. **a**, Experimental scheme. **b, c**, Representative dot plots showing depletion efficiency in the blood (**b**) and epithelium (**c**) of DQ8-D $^{d}$ -villin-IL-15tg mice after 30 days of anti-CD8 $\alpha$  treatment. **d, e**, Expression of Rae1 (**d**) and Qa-1 (**e**) genes

in the intestinal epithelium was determined by qPCR. Relative expression levels were normalized against the expression levels observed in sham-fed DQ8-D $^{d}$ -villin-IL-15tg mice (gluten + isotype,  $n=16$ ; gluten + anti-CD8,  $n=14$ ). **f**, Serum levels of anti-DGP IgG 30 days after gluten feeding ( $n=11$  mice per group). Data are mean  $\pm$  s.e.m. (**d, e**) or mean values (**f**) from four (**b–e**) or three (**f**) independent experiments. Pvalues determined by unpaired, two-tailed, t-test (**d–f**).

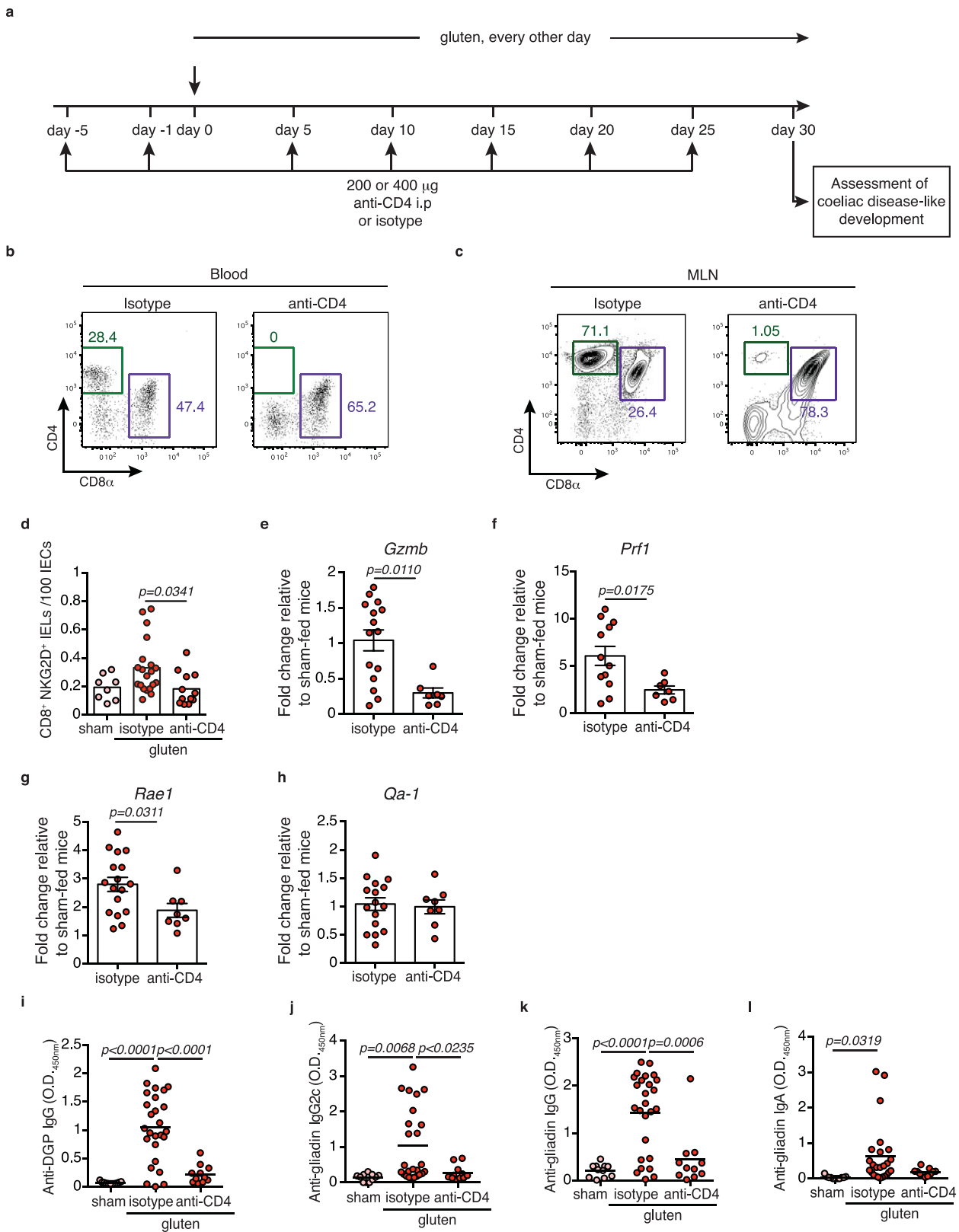


#### Extended Data Fig. 6 | HLA-DQ8 is required for the expansion of cytotoxic

**IELs.** **a**, Cells were isolated from the mesenteric lymph nodes of DQ8-D<sup>d</sup>-villin-IL-15tg and D<sup>d</sup>-villin-IL-15tg mice. CD11c<sup>+</sup>CD103<sup>+</sup> dendritic cells were analysed by flow cytometry for their expression of MHC class II and HLA-DQ8 molecules. **b–f**, DQ8-D<sup>d</sup>-villin-IL-15tg and D<sup>d</sup>-villin-IL-15tg mice raised on a GFD were maintained on a GFD or fed gluten for 30 days. **b**, Serum levels of anti-DGP IgG antibodies were measured by ELISA. Serum was collected 30 days after gluten feeding (DQ8-D<sup>d</sup>-villin-IL-15tg, sham  $n=17$ , gluten  $n=28$ ; D<sup>d</sup>-villin-IL-15tg, sham  $n=17$ , gluten  $n=28$ ). **c**, Expression of *Ifng* in the lamina propria was measured by qPCR. Relative expression levels in gluten groups were normalized against the expression levels observed in sham-fed DQ8-D<sup>d</sup>-villin-IL-15tg mice and sham-fed D<sup>d</sup>-villin-IL-15tg (DQ8-D<sup>d</sup>-villin-IL-15tg,  $n=8$ ; D<sup>d</sup>-villin-IL-15tg,  $n=9$ ). **d–f**, The

intestinal epithelium was isolated and analysed by flow cytometry. IELs were identified as TCR $\beta$ <sup>+</sup>CD4<sup>+</sup>CD8<sup>+</sup> cells. **d**, NKG2D<sup>+</sup>NKG2<sup>+</sup> IELs are indicated by absolute number per 100 IECs (DQ8-D<sup>d</sup>-villin-IL-15tg, sham  $n=8$ , gluten  $n=16$ ; D<sup>d</sup>-villin-IL-15tg, sham  $n=9$ , gluten  $n=22$ ). **e**, Granzyme B<sup>+</sup> IELs are indicated by absolute number per 100 IECs (DQ8-D<sup>d</sup>-villin-IL-15tg, sham  $n=8$ , gluten  $n=8$ ; D<sup>d</sup>-villin-IL-15tg, sham  $n=9$ , gluten  $n=10$ ). **f**, MFI of intracellular granzyme B (DQ8-D<sup>d</sup>-villin-IL-15tg, sham  $n=5$ , gluten  $n=6$ ; D<sup>d</sup>-villin-IL-15tg, sham  $n=5$ , gluten  $n=5$ ). Data are mean values (**b**, **d–f**) or mean  $\pm$  s.e.m. (**c**) from six (**b**, **d**), three (**c**), four (**e**) or two (**f**) independent experiments. *P* values were determined by ANOVA with Tukey's multiple comparison test (**b**, **d–f**) or unpaired, two-tailed, *t*-test (**c**).

# Article

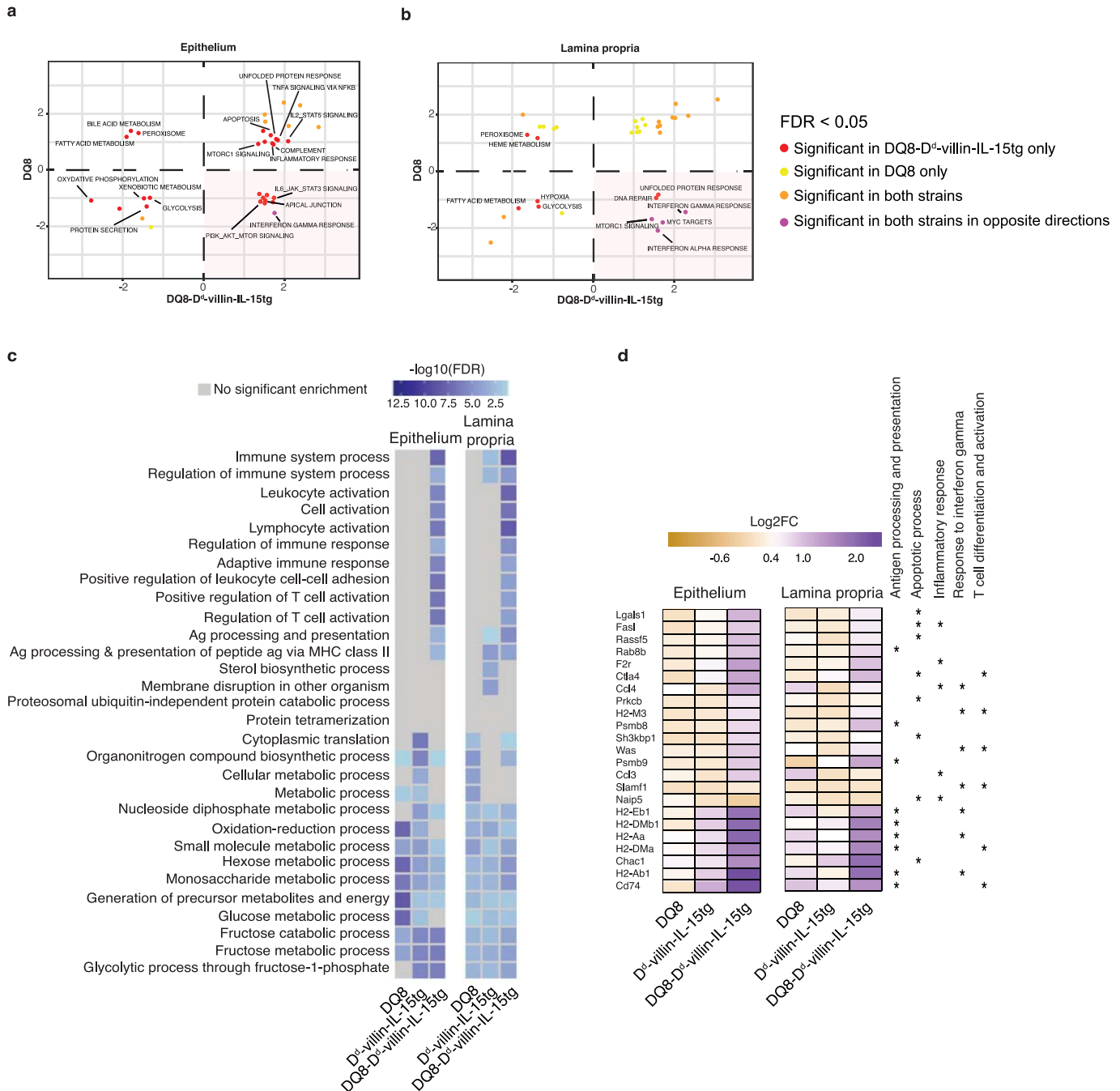


**Extended Data Fig. 7** | See next page for caption.

**Extended Data Fig. 7 | CD4<sup>+</sup> T cells are required for the pathogenesis of coeliac disease.** **a–l**, DQ8-D<sup>d</sup>-villin-IL-15tg mice were treated with 200 or 400 µg of depleting anti-CD4 antibody (clone GK1.5) or isotype control (rat IgG2b) twice before and during the course of gluten feeding. **a**, Experimental scheme. **b, c**, Representative dot plots showing depletion efficiency in the blood (**b**) and mesenteric lymph nodes (MLN) (**c**) of DQ8-D<sup>d</sup>-villin-IL-15tg mice. **d**, The intestinal epithelium was isolated and analysed by flow cytometry. IELs were identified as TCR $\beta$ <sup>+</sup>CD4<sup>+</sup>CD8<sup>+</sup> cells. NKG2D<sup>+</sup>NKG2<sup>−</sup>IELs are indicated by absolute number per 100 IECs. (sham,  $n$  = 8; gluten + isotype,  $n$  = 20; gluten + anti-CD4,  $n$  = 12). **e–h**, Expression of *Gzmb* (**e**), *Prf1* (**f**), *Rae1* (**g**) and *Qa-1* (**h**) in

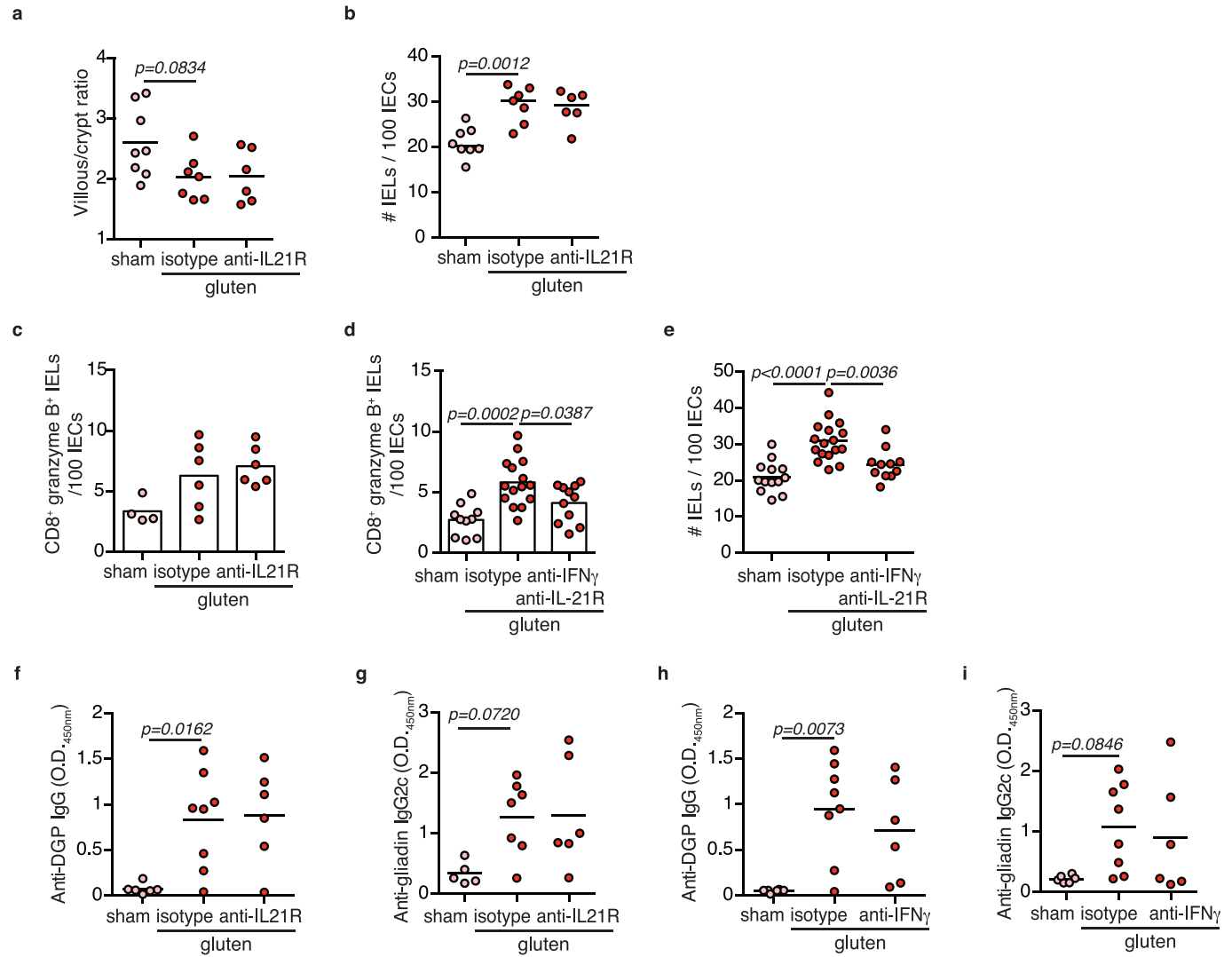
the intestinal epithelium as measured by qPCR. Relative expression levels were normalized against the expression levels observed in sham-fed DQ8-D<sup>d</sup>-villin-IL-15tg mice (gluten + isotype,  $n$  = 12 to 17; gluten + anti-CD4,  $n$  = 8). **i–l**, Serum levels of anti-DGP IgG (**i**), anti-gliadin IgG2c (**j**), anti-gliadin IgG (**k**) and anti-gliadin IgA (**l**) antibodies were measured by ELISA from serum collected 30 days after gluten feeding (sham,  $n$  = 11; gluten + isotype,  $n$  = 25–26; gluten + anti-CD4,  $n$  = 11). Data are mean values (**d, i–l**) or mean  $\pm$  s.e.m. (**e–h**) from four (**b–l**) independent experiments. *P* values determined by ANOVA with Tukey's multiple comparison test (**d, i–l**) or unpaired, two-tailed, *t*-test (**e–h**).

# Article



**Extended Data Fig. 8 | Transcriptional programs promoted by HLA-DQ8, IL-15 and gluten.** **a, b**, We contrasted the enrichment scores in the epithelium and the lamina propria for DQ8-D<sup>d</sup>-villin-IL-15tg (x axis) and DQ8 (y axis) mice for all pathways enriched at an FDR < 5% in at least one of the strains. Positive or negative scores represent enrichments among genes that are more highly or lowly expressed in gluten-fed mice, respectively. The bottom right quadrant refers to pathways that in response to gluten are upregulated in DQ8-D<sup>d</sup>-villin-

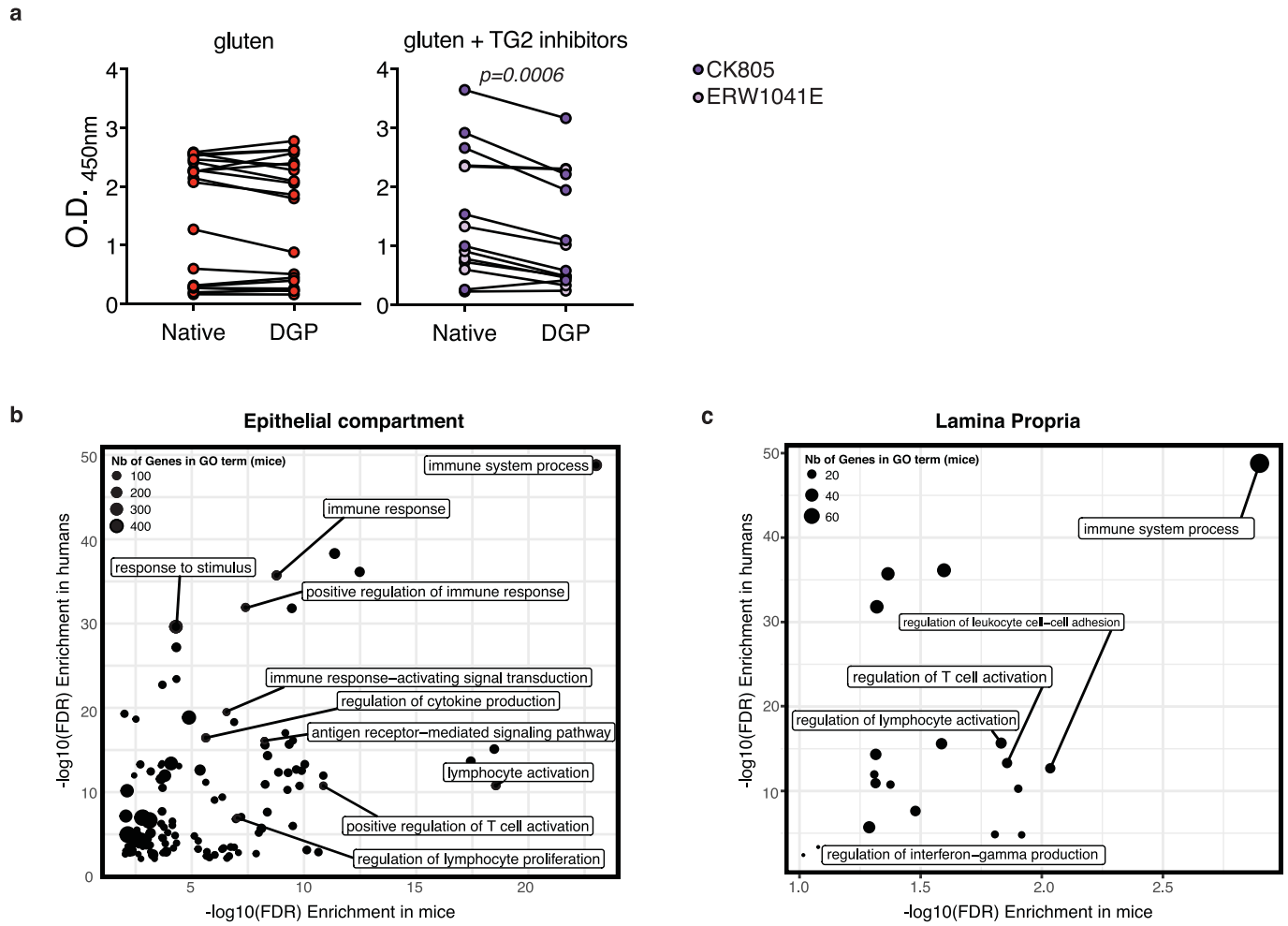
IL-15tg but downregulated in DQ8 mice. **c**, Gene Ontology terms significantly enriched among genes differently expressed in response to gluten challenge in DQ8, D<sup>d</sup>-villin-IL-15tg and DQ8-D<sup>d</sup>-villin-IL-15tg mice. **d**, Heat map of genes showing a stronger response to gluten in DQ8-D<sup>d</sup>-villin-IL-15tg mice as compared to DQ8 and D<sup>d</sup>-villin-IL-15tg mice. The colours reflect the magnitude of the response to gluten ( $\log_2$ -transformed scale), and the stars highlight Gene Ontology terms associated with each of the genes plotted.



**Extended Data Fig. 9 | Effect of IFN $\gamma$  and IL-21 neutralization on the development of coeliac disease.** **a–i**, DQ8-D<sup>d</sup>-villin-IL-15tg mice were treated with 500  $\mu$ g of anti-IFN $\gamma$  (clone XMG1.2) and/or anti-IL21R (clone 4A9) antibodies or corresponding isotype controls (rat IgG1 and rat IgG2a, respectively) once before, and every 3 days during the course of gluten feeding as indicated. **a**, Ratio of the morphometric assessment of villus height to crypt depth (sham,  $n$ =8, gluten + isotype,  $n$ =7, gluten + anti-IL21R,  $n$ =6). **b**, Quantification of IELs among IECs was performed on H&E-stained ileum sections (sham,  $n$ =8, gluten + isotype,  $n$ =7, gluten + anti-IL21R,  $n$ =6). **c**, The intestinal epithelium was isolated and analysed by flow cytometry. IELs were identified as TCR $\beta$ <sup>+</sup>CD4<sup>−</sup>CD8<sup>+</sup> cells. Granzyme B<sup>+</sup> IELs are indicated by absolute number per 100 IECs (sham,  $n$ =8, gluten + isotype,  $n$ =7, gluten + anti-IL21R,

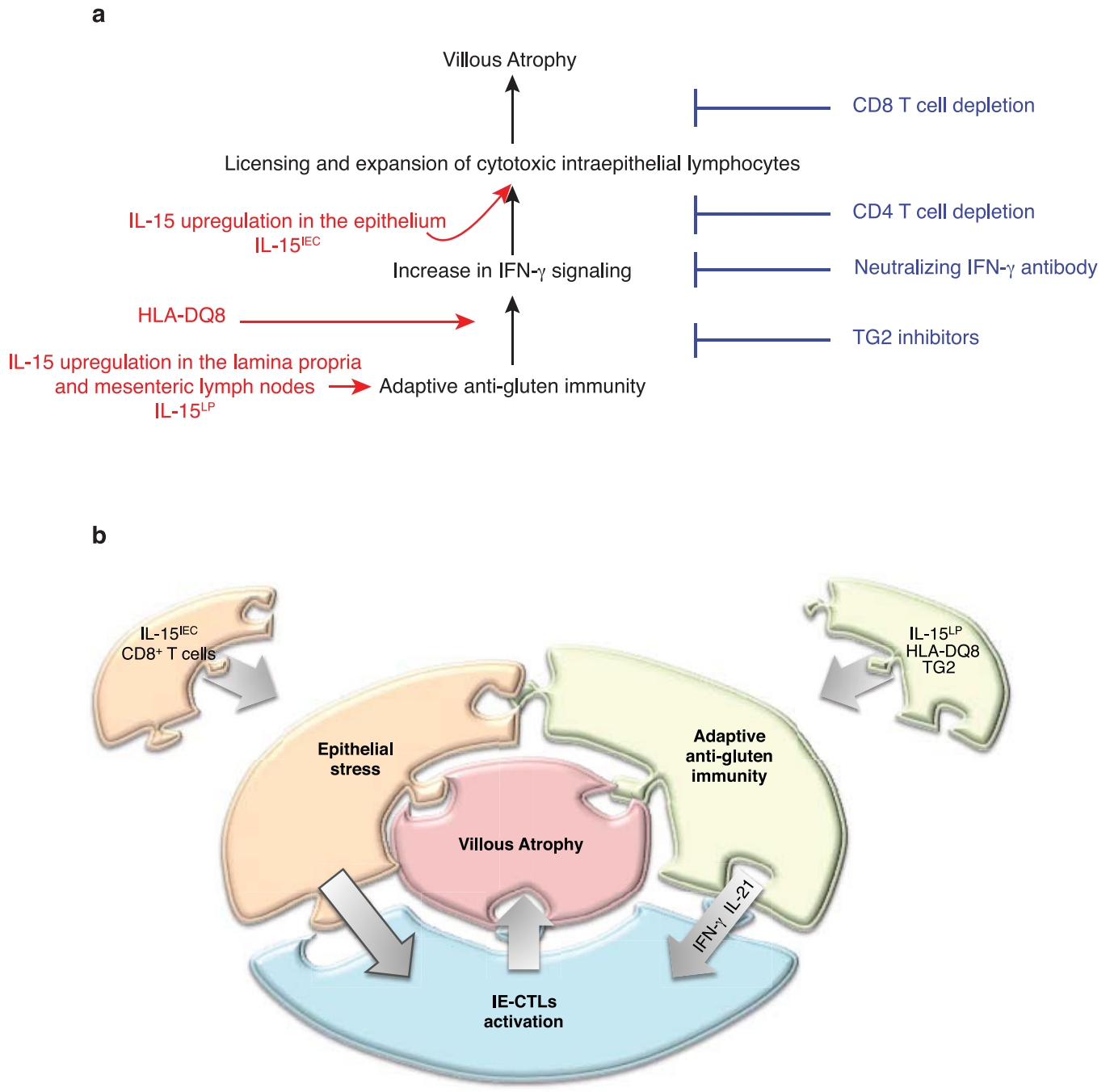
$n$ =6). **d**, Granzyme B<sup>+</sup> IELs are indicated as in **c** (sham,  $n$ =12, gluten + isotype,  $n$ =16, gluten + anti-IL21R + anti-IFN $\gamma$ ,  $n$ =11). **e**, Quantification of IELs among IECs was performed on H&E-stained ileum sections (sham,  $n$ =13, gluten + isotype,  $n$ =17, gluten + anti-IL21R + anti-IFN $\gamma$ ,  $n$ =11). **f**, **g**, Serum levels of anti-DGP IgG (**f**) and anti-gliadin IgG2c (**g**) antibodies were measured by ELISA. Serum was collected 30 days after gluten feeding (sham,  $n$ =5 and 6, gluten + isotype,  $n$ =8 and 7, gluten + anti-IL21R,  $n$ =6). **h**, **i**, Serum levels of anti-DGP IgG (**h**) and anti-gliadin IgG2c (**i**) antibodies were measured as in **f** and **g** (sham,  $n$ =6 and 6, gluten + isotype,  $n$ =8, gluten + anti-IFN $\gamma$ ,  $n$ =6). Data are mean values (**a–i**) from two (**a–c, f–i**) or four (**d, e**) independent experiments. *P* values determined by ANOVA with Tukey's multiple comparison test (**a–i**).

# Article



**Extended Data Fig. 10 | Validation of DQ8-D<sup>d</sup>-villin-IL-15tg mice as a preclinical mouse model of coeliac disease.** **a**, Serum anti-native gliadin peptides and anti-DGP IgG levels in gluten-fed DQ8-D<sup>d</sup>-villin-IL-15tg mice treated with TG2 inhibitors or vehicle (gluten) were compared by ELISA (gluten  $n=17$ ; gluten + TG2 inhibitors  $n=13$ ). In all cases, serum samples were obtained on day 30 after initiating the gluten challenge. **b**, Similar gene regulatory mechanisms underlie the development of coeliac disease in humans and DQ8-D<sup>d</sup>-villin-IL-15tg mice. Contrast between the Gene Ontology terms enriched among genes induced by gluten challenge in DQ8-D<sup>d</sup>-villin-IL-15tg mice

(depicted in the form of  $-\log_{10}(P\text{ values})$  on the x axis) and the Gene Ontology terms enriched among genes differently expressed between patients with coeliac disease and healthy controls (depicted in the form of  $-\log_{10}(P\text{ values})$  on the x axis) in the epithelial compartment (**a**) or the lamina propria (**b**). The transcriptional comparison was made between the intestinal epithelium and lamina propria of gluten-fed DQ8-D<sup>d</sup>-villin-IL-15tg mice and whole duodenal biopsies of patients with active coeliac disease. Data in **a** are mean values from four independent experiments. P value determined by paired, two-tailed, t-test).



**Extended Data Fig. 11 | Interplay between IL-15, TG2 and HLA-DQ8 promote the development of villous atrophy.** **a**, Representation of the respective roles of HLA-DQ8, IL-15, IFNy, TG2, CD4<sup>+</sup> and CD8<sup>+</sup> T cells in promoting villous atrophy. IL-15 upregulation in the lamina propria is required to induce the adaptive anti-gluten T<sub>H</sub>1 response, and HLA-DQ8 facilitates and enhances the IFNy response that is required for the development of villous atrophy. However, the adaptive T<sub>H</sub>1 immune response promoted by HLA-DQ8 and IL-15 in the lamina propria is insufficient to cause tissue destruction. It needs to synergize with IL-15 in the epithelium to further promote the expansion of cytolytic IELs

and their degranulation, leading to CD8<sup>+</sup> T cell-dependent killing of epithelial cells and villous atrophy. The value of this mouse model as a gluten- and HLA-DQ8-dependent pre-clinical model for coeliac disease is further emphasized by the finding that TG2 inhibition prevents villous atrophy. **b**, Coeliac disease can be represented as a jigsaw puzzle in which each piece representing one component of the anti-gluten immune response must interlock to lead to the development of villous atrophy—the diagnostic hallmark of active coeliac disease.

# Reporting Summary

Nature Research wishes to improve the reproducibility of the work that we publish. This form provides structure for consistency and transparency in reporting. For further information on Nature Research policies, see [Authors & Referees](#) and the [Editorial Policy Checklist](#).

## Statistics

For all statistical analyses, confirm that the following items are present in the figure legend, table legend, main text, or Methods section.

n/a Confirmed

- The exact sample size ( $n$ ) for each experimental group/condition, given as a discrete number and unit of measurement
- A statement on whether measurements were taken from distinct samples or whether the same sample was measured repeatedly
- The statistical test(s) used AND whether they are one- or two-sided  
*Only common tests should be described solely by name; describe more complex techniques in the Methods section.*
- A description of all covariates tested
- A description of any assumptions or corrections, such as tests of normality and adjustment for multiple comparisons
- A full description of the statistical parameters including central tendency (e.g. means) or other basic estimates (e.g. regression coefficient) AND variation (e.g. standard deviation) or associated estimates of uncertainty (e.g. confidence intervals)
- For null hypothesis testing, the test statistic (e.g.  $F$ ,  $t$ ,  $r$ ) with confidence intervals, effect sizes, degrees of freedom and  $P$  value noted  
*Give  $P$  values as exact values whenever suitable.*
- For Bayesian analysis, information on the choice of priors and Markov chain Monte Carlo settings
- For hierarchical and complex designs, identification of the appropriate level for tests and full reporting of outcomes
- Estimates of effect sizes (e.g. Cohen's  $d$ , Pearson's  $r$ ), indicating how they were calculated

*Our web collection on [statistics for biologists](#) contains articles on many of the points above.*

## Software and code

Policy information about [availability of computer code](#)

Data collection

Raw microarray data were processed by GenomeStudio (illumina, GSGX Version 1.9.0). FACs DIVA software was used for flow cytometry data collection. ELISA raw data were processed with SkanIt Software for Multiskan Go (Thermo Scientific). Slides were analyzed using the Las X software (Leica)

Data analysis

For RNA-seq analysis, Trim Galore (version 0.2.7), Kallisto v0.43.0, Gene transcriptional analysis was performed in R using the bioconductor limma package. Gene ontology enrichment analysis were performed in Gorilla. FlowJo, GraphPad Prism, Excel, ImageJ were used for the other analyses. Slides were analyzed using Image J. Flow cytometry data were analyzed using FlowJo, GraphPad Prism, and Excel.

For manuscripts utilizing custom algorithms or software that are central to the research but not yet described in published literature, software must be made available to editors/reviewers. We strongly encourage code deposition in a community repository (e.g. GitHub). See the Nature Research [guidelines for submitting code & software](#) for further information.

## Data

Policy information about [availability of data](#)

All manuscripts must include a [data availability statement](#). This statement should provide the following information, where applicable:

- Accession codes, unique identifiers, or web links for publicly available datasets
- A list of figures that have associated raw data
- A description of any restrictions on data availability

Data are available upon request from the corresponding authors.

# Field-specific reporting

Please select the one below that is the best fit for your research. If you are not sure, read the appropriate sections before making your selection.

Life sciences       Behavioural & social sciences       Ecological, evolutionary & environmental sciences

For a reference copy of the document with all sections, see [nature.com/documents/nr-reporting-summary-flat.pdf](http://nature.com/documents/nr-reporting-summary-flat.pdf)

## Life sciences study design

All studies must disclose on these points even when the disclosure is negative.

Sample size	The majority of experiments were repeated at least three times to obtain data for indicated statistical analyses. Mice were allocated to experimental groups on the basis of their genotype and randomized within the given age-matched group. Given that our mice were inbred and matched for age, we always assumed similar variance between the different experimental group. We did not perform an a priori sample size estimation but always used as many mice per group as possible in an attempt to minimize type I and type II errors.
Data exclusions	There were no data exclusions.
Replication	All attempts at replication were successful. Several experiments were pooled to take into account the variation inherent to the model.
Randomization	Mice were allocated to experimental groups on the basis of their genotype and randomized within given sex- and age-matched groups.
Blinding	Investigators were not blinded during experiments and outcome assessments as different groups of mice (receiving different diets or treatments) were processed in parallel and had to be clearly identified to prevent errors and cross-contamination. At least two investigators were blinded for the detection of anti-DGP antibodies by ELISA and the microscopic analysis of the incidence of villous atrophy and the determination of villous to crypt ratio.

## Reporting for specific materials, systems and methods

We require information from authors about some types of materials, experimental systems and methods used in many studies. Here, indicate whether each material, system or method listed is relevant to your study. If you are not sure if a list item applies to your research, read the appropriate section before selecting a response.

Materials & experimental systems		Methods
n/a	Involved in the study	n/a
<input type="checkbox"/>	<input checked="" type="checkbox"/> Antibodies	<input checked="" type="checkbox"/> ChIP-seq
<input checked="" type="checkbox"/>	<input type="checkbox"/> Eukaryotic cell lines	<input type="checkbox"/> <input checked="" type="checkbox"/> Flow cytometry
<input checked="" type="checkbox"/>	<input type="checkbox"/> Palaeontology	<input checked="" type="checkbox"/> <input type="checkbox"/> MRI-based neuroimaging
<input type="checkbox"/>	<input checked="" type="checkbox"/> Animals and other organisms	
<input type="checkbox"/>	<input checked="" type="checkbox"/> Human research participants	
<input type="checkbox"/>	<input type="checkbox"/> Clinical data	

## Antibodies

Antibodies used	<p>For flow cytometry, the following antibodies were used (company, catalog number, clone):</p> <p>TCRb APC (eBioscience, 11-5961-82, H57-597), CD8a APC-eFluor 780 (eBioscience, 47-0081-82, 53-6.7), CD8b PE-Cy5 (eBioscience, 15-0083-81, eBioH35-17.2), CD314 (NKG2D) PE (eBioscience, 12-5882-82, CX5), NKG2AB6 PE (eBioscience, 12-5897-81.16a11), CD94 FITC (eBioscience, 11-0941-82, 18d3), CD11c PE (eBioscience, 12-0114-82, N418), CD4 PE-Cy7 (BD Biosciences, 563933, GK1.5), CD4 BV711 (BD Biosciences, 563050, GK1.5), CD103 APC (BD Biosciences, 562772, M290), NKG2A/C/E FITC (BD Biosciences, 550520, 20d5), CD3FITC (BD Biosciences, 555274, 17A2), CD3 BUV737 (BD Biosciences, 612803, 17A2), IgA FITC (BD Biosciences, 559354, C10-3), CD16/CD32 (BD Biosciences, 553142, 2.4G2), CD107a FITC (BD Biosciences, 561069, 1D4B). HLA-DQ8 PE (BioLegend, 318106, HLADQ81), CD11c BV421 (BioLegend, 117343, N418), CD3PE/Cy7 (BioLegend, 100320, 145-2c11), Ep-CAM PerCP/Cy5.5 (BioLegend, 118220, G8.8), F4/80 PE(BioLegend, 123110, BM8), NK1.1(BioLegend, 108707, PK136) and CD45 Pacific Blue (BioLegend, 103126, 30-F11), Rae1 AF647 (R&amp;D Systems, FAB1135R), Granzyme B PE (Invitrogen, MHGB04, GB12), I-Ab FITC (eBioscience, 11-5321-81, M5/114.15.2), CD8 APC-eFluor 780 (eBioscience, 47-0081-82, 53-6.70), B220 PE-Cyanine7 (eBioscience, 25-0452-82, RA3-6B2) and LIVE/DEAD™ Fixable Violet Dead Cell Stain Kit (Invitrogen, L34963). For in vivo neutralization experiments, the following antibodies were used: anti-CD4 (BioXCell, BE0003-1, GK1.5), anti-CD8α (BioXCell, BE0061, 2.43), anti-IFN-gamma (BioXCell, BE0055, XMG1.2), anti-IL-21R (BioXCell, BE0258, 4A9), RatIgG2b isotype control (BioXCell, BE0090, LTF-2), rat IgG1 isotype control (BioXCell, BE0088, HRPN), or RatIgG2a (BioXCell, BE0089, 2A3).</p> <p>For ELISA, the following antibodies were used:</p> <p>Goat anti-mouse Ig-horseradish peroxidase (HRP) (Southern Biotech, polyclonal, 1030-05, K3515-T5661), goat anti-mouse IgA horseradish peroxidase (HRP) (Southern Biotech, 1040-05), goat anti-mouse IgG-horseradish peroxidase (HRP) (Southern Biotech, 1079-05), goat anti-mouse IgG biotin conjugate (Jackson Immunoresearch, 115-065-003), streptavidin-HRP (Jackson</p>
-----------------	---

(Immunoresearch, 016-030-084).

For immunofluorescence staining, the following antibodies were used: purified anti-mouse CD138 (BD Biosciences, 553712, 281-2), Alexa Fluor 594 anti-mouse CD3 (Biolegend, 100240, 17A2), anti-mouse IgA-biotin (Southern Biotech, 1165-08, 11-44-2), anti-transglutaminase 2 (rabbit polyclonal, Pacific Immunology), goat anti-rat IgG Alexa Fluor 488 (Invitrogen Molecular Probes, A-11006), goat anti-rat IgG Alexa Fluor 633 (Invitrogen Molecular Probes, A-21094), Alexa Fluor 594 streptavidin (Invitrogen Molecular Probes, S11227), goat anti-rabbit Alexa Fluor 488 (Molecular Probes, A-11070).

For histology staining, the following antibodies were used: polyclonal goat IgG anti-mouse Granzyme B (R&D Systems, AF1865), biotinylated anti-goat IgG (Vector Laboratories, BA-5000).

## Validation

All antibodies are commercially available and have been validated by manufacturers and in previous publications.

## Animals and other organisms

Policy information about [studies involving animals](#); [ARRIVE guidelines](#) recommended for reporting animal research

### Laboratory animals

Mice used in these studies are on the C57BL/6 background. Mice were maintained under specific pathogen-free conditions at the University of Chicago and at the Sainte-Justine University Hospital Research Center. Importantly, no differences in the outcome of the experiments were observed between the two institutions, enabling to pool the data. HLA-DQ8 transgenic mice (DQ8) and DQ8-Dd-IL-15tg mice expressing IL-15 under the minimal MHC class I Dd promoter were previously described (see References in the manuscript). Villin-IL-15tg mice expressing IL-15 under the intestine-specific villin promoter of IECs (see reference in the manuscript) were crossed to HLA-DQ8 mice (DQ8-villin-IL-15tg in the present manuscript). DQ8-Dd-IL-15tg mice were then crossed onto DQ8-villin-IL-15tg mice to obtain the first generation DQ8-Dd-villin-IL-15tg mice. Next generations were obtained by backcrossing DQ8-Dd-villin-IL-15tg mice with DQ8-villin-IL-15tg mice. Finally DQ8-Dd-villin-IL-15tg mice were crossed to Dd-IL-15tg or villin-IL-15tg mice to obtain Dd-villin-IL-15tg mice. All strains were maintained on a gluten-free chow (AIN76A, Envigo). Both female and male mice were used for experiments and no notable sex-dependent differences were found for the reported experiments. For all experiments, mice were used at 10 weeks of age.

### Wild animals

This study did not involve wild animals.

### Field-collected samples

This study did not involve samples collected from the field.

### Ethics oversight

All experiments were performed in accordance with the Institutional Biosafety Committee and the Institutional Care and Use Committee of the University of Chicago, and with the Canadian Council on Animal Care guidelines and the Institutional Committee for Animal Care in Research of the Sainte-Justine University Hospital Research Center.

Note that full information on the approval of the study protocol must also be provided in the manuscript.

## Human research participants

Policy information about [studies involving human research participants](#)

### Population characteristics

96 individuals undergoing upper gastrointestinal endoscopy during diagnostic work-up at the University of Chicago Medicine and at Mayo Clinic, including 45 non-coeliac controls (29 females and 16 males) and 51 untreated Coeliac disease patients (31 females and 20 males) were recruited.

### Recruitment

Patients were approached by our clinical coordinator in the endoscopy clinic and were asked to read the specific terms detailed in the informed consent form before consenting to participate to the study. Control subjects underwent upper gastrointestinal endoscopy during a diagnostic work-up for anemia, failure to thrive or other intestinal disorders not associated with coeliac disease. All controls had normal small intestinal histology, no family history of coeliac disease, no significant levels of anti-TG2 IgA antibodies in the serum. Active coeliac disease patients all had positive anti-TG2 antibodies and small intestinal enteropathy with increased infiltration of intraepithelial lymphocytes, crypts hyperplasia and villous atrophy.

### Ethics oversight

Each subject signed an informed consent as provided by the Institutional Review Board of each institution (IRB-12623B for the University of Chicago and IRB-1491-03 for Mayo Clinic).

Note that full information on the approval of the study protocol must also be provided in the manuscript.

## Flow Cytometry

### Plots

Confirm that:

- The axis labels state the marker and fluorochrome used (e.g. CD4-FITC).
- The axis scales are clearly visible. Include numbers along axes only for bottom left plot of group (a 'group' is an analysis of identical markers).
- All plots are contour plots with outliers or pseudocolor plots.
- A numerical value for number of cells or percentage (with statistics) is provided.

## Methodology

### Sample preparation

Single cells suspension were obtained from the gut epithelium, mesenteric lymph nodes, and blood. Intestinal epithelial cells were isolated by incubating gut fragments at 37°C under agitation in EDTA containing calcium-free RPMI medium. A cell purification step using a 40% Percoll was used to enrich lymphocyte cell populations for flow cytometry analysis. Mesenteric lymph nodes were dissected, and made into a single cell suspension by mechanical disruption and passed through a 70µm nylon cell strainer. After collection of peripheral blood, erylysis was performed using the BD FACS lysing solution.

### Instrument

Flow Cytometry analysis was performed on a BD LSRFortessa II cell analyzer (BD Biosciences).

### Software

FACSDIVA software (BD Biosciences) was used to collect flow cytometry data and FlowJo software (Treestar) was used to analyze them.

### Cell population abundance

Not applicable.

### Gating strategy

All samples are FSC-A and SSC-A gated, followed by Live/Dead gating to select viable cells. Subsequent relevant gating was conducted as shown in figures and described in figure legends.

Tick this box to confirm that a figure exemplifying the gating strategy is provided in the Supplementary Information.